Regional heterogeneities in the emission of airborne primary sugar compounds and biogenic secondary organic aerosols in the East Asian outflow: Evidence for coal combustion as a source of levoglucosan

M. Mozammel Haque[1,2,3], Yanlin Zhang[1,2*] Srinivas Bikkina[4], Meehye Lee[5], and Kimitaka Kawamura[3,4*]

[1]Yale-NUIST Center on Atmospheric Environment, International Joint Laboratory on Climate and Environment Change (ILCEC), Nanjing University of Information Science & Technology, Nanjing, 210044, China
[2]School of Applied Meteorology, Nanjing University of Information Science & Technology, Nanjing 210044, China
[3]Institute of Low Temperature Science, Hokkaido University, Sapporo 060-0819, Japan
[4]Chubu Institute for Advanced Studies, Chubu University, Kasugai 487-8501, Japan
[5]Department of Earth and Environmental Sciences, Korea University, Anam-dong, Sungbuk-gu, Seoul 136-701, South Korea

**Corresponding author*
E-mail: dryanlinzhang@outlook.com (Yan-Lin Zhang)
E-mail: kkawamura@isc.chubu.ac.jp (Kimitaka Kawamura)

ABSTRACT

Biomass burning (BB) significantly influences the chemical composition of organic aerosols (OA) in the East Asian outflow. Source apportionment of BB-derived OA is an influential factor for understanding their regional emissions, which is crucial for reducing uncertainties in their projected climate and health-effects. We analyzed here three different classes of atmospheric sugar compounds (anhydrosugars, primary sugars, and sugar alcohols) and two types of biogenic secondary organic aerosol (BSOA) tracers (isoprene- and monoterpene derived SOA products) in a year-long collected total suspended particulate matter (TSP) from an island-based receptor site in South Korea, the Gosan. We investigate seasonal variations in the source-emissions of BB-derived OA using mass concentrations of anhydrosugars and radiocarbon (^{14}C-) isotopic composition of organic carbon (OC) and elemental carbon (EC) in ambient aerosols. Levoglucosan (*Lev*) is the most abundant anhydrosugar, followed by galactosan (*Gal*) and mannosan (*Man*). Strong correlations of *Lev* with *Gal* and *Man*, along with their ratios (*Lev*/*Gal:* 6.65 ± 2.26; *Lev*/*Man*: 15.1 ± 6.76) indicate the contribution from hardwood burning emissions. The seasonal trends revealed that the BB impact is more pronounced in winter and fall, as evidenced by the high concentrations of anhydrosugars. Likewise, significant correlations among three primary sugars (i.e., glucose, fructose, and sucrose) emphasized the contribution of airborne pollen. The primary sugars showed higher concentrations in spring/summer than winter/fall. The fungal spore tracer compounds (i.e., arabitol, mannitol, and erythritol) correlated well with trehalose (i.e., a proxy for soil organic carbon), suggesting the origin from airborne fungal spores and soil microbes in the East Asian outflow. These sugar alcohols peaked in summer, followed by spring/fall and winter. Monoterpene-derived SOA tracers were most abundant compared to isoprene-SOA tracers. Both BSOA tracers were dominant in summer, followed by fall, spring, and winter. The source apportionment based on multiple linear regressions, diagnostic mass ratios, and positive matrix factorization analysis altogether revealed that biomass burning (41.9%) and biogenic SOA (21.1%) mostly dictate the OA loading in the ambient aerosols from East Asian outflow. We also found significant positive linear relationships of ^{14}C-based nonfossil- and fossil-derived organic carbon fractions with *Lev-C* along with the comparable regression slopes, suggesting the importance of BB and coal combustion sources in the East Asian outflow.

Keywords: Biomass burning tracers, primary biological aerosol particles, biogenic SOA tracers, radiocarbon-based source apportionment, organic aerosols, East Asian outflow

1. Introduction

Organic aerosols (OA), which account for a major fraction of up to 50% of airborne total suspended particulate matter, have considerable effects on regional and global climate by absorbing or scattering sunlight (Kanakidou et al., 2005). However, the climate effects of OA are involved with large uncertainties due to our limited understanding of the contributing sources. OA can be derived from both primary emissions and secondarily formed species. Sugars are an important group of water-soluble, primarily organic compounds whose concentrations are significant in atmospheric aerosols over the continent (Jia and Fraser, 2011; Fu et al., 2008; Yttri et al., 2007; Graham et al., 2003). Anhydrosugars such as levoglucosan, galactosan, and mannosan are the key tracers of biomass burning (BB) emissions (Simoneit, 2002). Sugar alcohols, along with glucose, trehalose and sucrose are mostly originated from primary biological particles such as fungal spores, pollen, bacteria, and viruses, and vegetative debris (Graham et al., 2003; Simoneit et al., 2004a; Bauer et al., 2008; Deguillaume et al., 2008). Primary sugars and sugar alcohols are predominantly present in the coarse mode aerosols, accounting for 0.5-10% of atmospheric aerosol carbon matter (Yttri et al., 2007; Pio et al., 2008).

Secondary organic aerosol (SOA) is a large fraction of OA, while there were only limited studies about the key factors controlling SOA formation. The SOA formation significantly increased with the enhancement of the ambient aerosol mass (Liu et al., 2018). SOA is formed by both homogenous and heterogeneous reactions of volatile organic compounds (VOCs) in the atmosphere (Surratt et al., 2010; Robinson et al., 2007; Claeys et al., 2004). On a global estimation, biogenic VOCs (BVOCs) such as isoprene, monoterpenes (e.g., α/β-pinene), and sesquiterpenes (e.g., β-caryophyllene) are one order of magnitude higher than those of anthropogenic VOCs (e.g., toluene) (Guenther et al., 2006). The global emissions of annual BVOCs were estimated to be 1150 TgC yr^{-1}, accounting for 44% isoprene and 11% monoterpenes (Guenther et al., 1995). Isoprene is highly reactive and promptly reacts with oxidants such as O_3, OH, and NO_x in the atmosphere to form SOA (Kroll et al., 2005, 2006; Ng et al., 2008; Surratt et al., 2010; Bikkina et al., 2021), estimated to be 19.2 TgC yr^{-1}, consisting of ~70% of the total SOA budget (Heald et al., 2008). Monoterpenes are important sources of biogenic secondary organic aerosol (BSOA), accounting for ~35% of the global BVOCs emissions (Griffin et al., 1999).

Anthropogenic activities such as coal and biofuel combustion over East Asia, including China, are responsible for the vast emission of OA (Huebert et al., 2003; Zhang et al., 2016). Understanding the ambient levels OA in the East Asian outflow is crucial for

assessing their regional climatic effects. As part of this effort, Korean Climate Observatory at Gosan (KCOG), a super site located in South Korea, is an ideal location for investigating the atmospheric outflow characteristics from East Asia (Fu et al., 2010a; Kundu et al., 2010; Ramanathan et al., 2007; Kawamura et al., 2004; Arimoto et al., 1996). For instance, primary OA associated with soil/desert dust in East Asia, along with forest fires in Siberia/northeastern China, are transported over Gosan in spring (Wang et al., 2009a). BSOA during long-range transport from the continent and Open Ocean, as well as local vegetation, can significantly contribute to Gosan aerosols. Although these investigations were carried out almost a decade ago, no such observations are available in contemporary times from Gosan. Here, we attempt to understand the current states of East Asian OA using both the molecular marker approach and radiocarbon data of carbonaceous components.

The KCOG, located on the western side of Jeju Island adjacent to the Yellow Sea and the East China Sea, is facing the Asian continent but is isolated from public areas of the island (Kawamura et al., 2004). Simoneit et al. (2004b) have documented during the ACE-Asia campaign that OA from the BB and fossil fuel combustion sources are transported along with desert dust to the KCOG during continental outflow. An intensive campaign was organized at the KCOG during spring 2005 to observe the physical properties of East Asian aerosols while two dust events were detected (Nakajima et al., 2007). Here, we focus on the characterization of airborne anhydrosugars, primary sugars, sugar alcohols, and BSOA tracers from the KCOG. Gosan is influenced by the continental outflow from East Asia during winter, spring and fall, whereas the site is influenced by the maritime air masses from the Pacific Ocean and other marginal seas. This makes the KCOG ideal for characterizing the regional heterogeneities in the emissions of organic compounds in the East Asian outflow based on the TSP samples collected during April 2013-April 2014.

2. Methods

2.1. Aerosol sampling and prevailing meteorology

Total suspended particles (TSP) were collected on pre-combusted (450°C for 6 h) quartz fiber filters (20 cm × 25 cm, Pallflex) at the KCOG (33.17 °N, 126.10 °E, see Figure 1), South Korea. To get enough signal for the radiocarbon measurements, each TSP sample was collected for 10–14 days from April 2013 to April 2014. Twenty-one samples were collected using a high-volume air sampler (Kimoto AS-810, ~65 m^3 h^{-1}) installed on the rooftop of a trailer house (~3 m above the ground). After the collection, aerosol filters were transferred to a pre-combusted (450°C for 6 h) glass jar (150 mL) equipped with a Teflon-lined screw cap and transported to the laboratory in Sapporo. These TSP samples were stored in a dark

freezer room at -20°C until the analysis. Three field blank filters were also collected during the campaign.

The ambient temperatures at the Gosan site were on average 6.9°C in winter, 14.1°C in spring, 27.0°C in summer, and 17.1°C in fall. Likewise, the average relative humidity was found to be highest in summer (71.3%), followed by spring (64.9%), fall (63.5%), and winter (54.7%). Gosan is influenced by the pollution sources in East Asia during winter as well as other transition periods (spring and fall) due to the prevailing westerlies. In contrast, winds in summer blew mostly from the western North Pacific (WNP) by the easterly winds. The spring season is, in particular, important for the transport of mineral dust mixed with polluted OA to Gosan (Kundu et al., 2010).

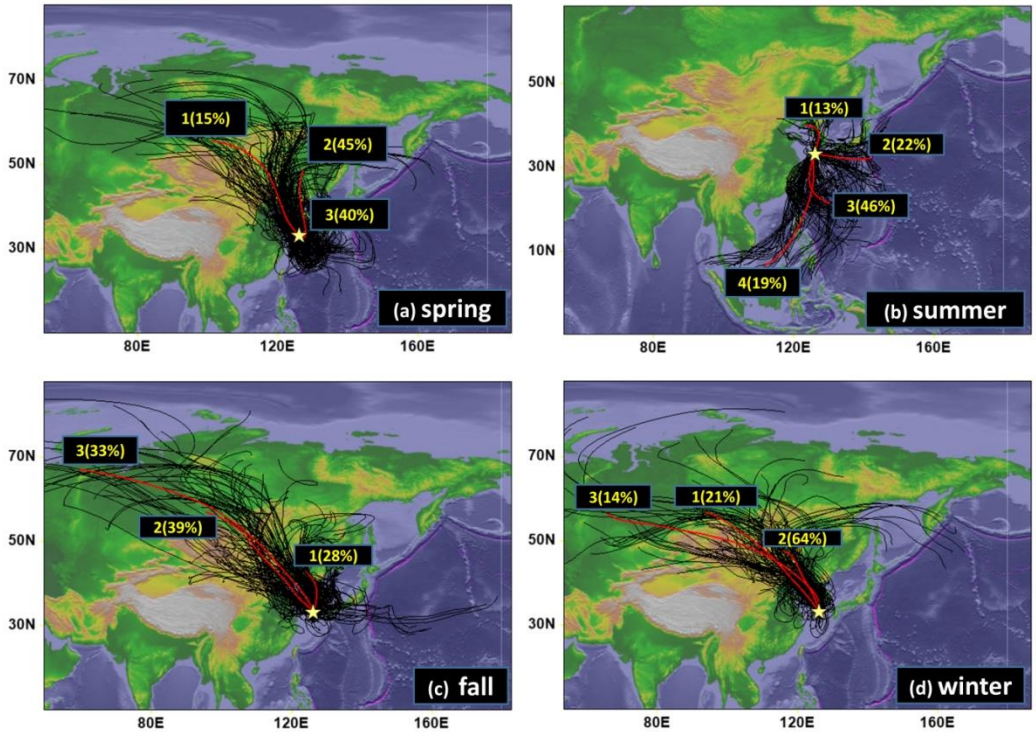

Figure 1. Cluster analysis of backward air mass trajectories over Gosan (indicated by a star symbol) for the TSP collected during (a) spring, (b) summer, (c) fall, and (d) winter seasons.

2.2. Extraction and analysis of organic compounds

Approximately 3.14 cm^2 filter cuts were extracted with dichloromethane/methanol (2:1; v/v). The extracts were concentrated using a rotary evaporator under vacuum and then blown down to near dryness with pure nitrogen gas. The dried residues were subsequently reacted with N, O-bis(trimethylsilyl)trifluoroacetamide containing 1% trimethylchlorosilane (BSTFA+1%

TMCS, SUPELCO©, Sigmaaldrich®) and pyridine at 70 °C for 3 h to derive OH and COOH groups of polar organic compounds to trimethylsilyl ethers and esters, respectively. After the derivatization followed by the addition of a known amount of internal standard solution (Tridecane; 1.43 ng L^{-1} in n-hexane), the derivatized extracts were injected onto a gas chromatograph (Hewlett-Packard model 6890 GC) coupled to a mass spectrometer (Hewlett-Packard model 5973, MSD) (GC-MS). More details on the quantification of polar organic compounds using GC-MS are described in Haque et al. (2019).

The target compounds (anhydrosugars, primary sugars, sugar alcohols, and BSOA tracers) were separated on a DB-5MS fused silica capillary column (30 m x 0.25 mm i.d., 0.5 μm film thickness) using helium as a carrier gas at a flow rate of 1.0 ml min^{-1}. The GC oven temperature was programmed from 50°C for 2 min and then increased from 50 to 120°C at 30°C min^{-1} and to 300°C at 6°C min^{-1} with a final isotherm hold at 300°C for 16 min. The sample was injected in a splitless mode with the injector temperature at 280°C. The MS was operated at 70 eV and scanned from 50 to 650 Da on an electron impact (EI) mode. Mass spectral data were acquired and processed using the Chemstation software. The organic compounds were identified individually by comparison with retention times and mass spectra of authentic standards and NIST library and literature data of mass fragmentation patterns (Medeiros and Simoneit, 2007). For assessing the recoveries, ~100-200 ng of the standard solution was spiked on the blank filter and analyzed as a real sample. Overall, the average recoveries were found to be 80-104% for target compounds. The field and laboratory blank filters (n = 3) were also analyzed by the same procedures as a real sample. Target compounds were not found in the field blanks. The analytical errors based on concentrations by replicate sample analyses (n = 3) were less than 15%.

2.3. Radiocarbon isotopic composition of TC and EC

The concentrations of total carbon (TC) in TSP samples were analyzed using an elemental analyzer. For the radiocarbon isotopic composition ($\Delta^{14}C$), the aerosol filter punches were exposed for ~12 h to HCl fumes in a vacuum desiccator. Subsequently, these filters were analyzed for $\Delta^{14}C$ on a modified elemental analyzer coupled via a gas interface to Accelerator Mass Spectrometer Mini Carbon Dating System (MICADAS) at the University of Bern, Switzerland (Salazar et al., 2015). The evolved CO_2 of TC from the elemental analyzer was passed through a moisture trap (Sicapent, Merck) and isolated it from other residual gasses using a temperature-controlled zeolite trap. The purified CO_2 was introduced through a gas interface system to MICADAS, where $^{14}C/^{12}C$ ratios are measured according to the analytical

196 procedures detailed in Zhang et al. (2016). Likewise, the evolved CO_2 of elemental carbon
197 from the Sunset Lab OC/EC analyzer using Swiss 4S protocol (Zhang et al., 2012), was
198 directed to the MICDAS and measured for the $^{14}C/^{12}C$ ratio relative to standard calibration
199 gas. These results were expressed as fractions of modern carbon (f_M) by normalizing with a
200 $\delta^{13}C$ value of the reference standard in the year 1950 (–25‰) according to Stuiver and Polach
201 (1997) for the fractionation effects. The f_M(OC) can be estimated by using the f_M(TC) and
202 f_M(EC) in an isotope mass balance equation (Zhang et al., 2015). Additionally, we estimated
203 the relative contributions of OC and EC from the nonfossil and fossil sources ($f_{nonfossil}$ and
204 f_{fossil}, respectively) using the following equations.

205 $$f_{nonfossil\text{-}OC} = f_M(\text{OC-sample})/f_M(\text{OC-ref});\ f_M(\text{OC-ref}) \approx 1.07\pm0.04 \quad (1)$$

206 $$f_{nonfossil\text{-}EC} = f_M(\text{EC-sample})/f_M(\text{EC-ref});\ f_M(\text{EC-ref}) \approx 1.10\pm0.05 \quad (2)$$

207 $$f_{fossil\text{-}OC} = 1 - f_{nonfossil\text{-}OC} \quad (3)$$

208 $$f_{fossil\text{-}EC} = 1 - f_{nonfossil\text{-}EC} \quad (4)$$

209 The reference values of OC and EC were obtained from Mohn et al. (2008). Using
210 the fractions of $f_{fossil\text{-}OC}$ and $f_{nonfossil\text{-}OC}$, we can, therefore, estimate the mass concentration of
211 ambient organic carbon (OC-ambient) from fossil and nonfossil sources (OC_{fossil} and
212 $OC_{nonfossil}$, respectively).

213 $$OC_{nonfossil} = f_{nonfossil\text{-}OC} \times [OC]_{ambient} \quad (5)$$

214 $$OC_{fossil} = f_{fossil\text{-}OC} \times [OC]_{ambient} \quad (6)$$

215 More details on the radiocarbon isotopic composition data over Gosan were reported
216 elsewhere (Zhang et al., 2016).

217 **3. Results and discussion**

218 **3.1. Trajectory and cluster analysis**

219 Backward air mass trajectories are useful for assessing the impact of local versus regional
220 source emissions over Gosan. Seven-day isentropic backward air mass trajectories were
221 computed using the hybrid single-particle Lagrangian integrated trajectory model (HYSPLIT,
222 version 4: Stein et al., 2015) over the KCOG for the sampling period using the
223 meteorological datasets of the Global Data Assimilation System (GDAS) network. The
224 trajectory endpoint files from the HYSPLIT model were further used for the cluster analysis
225 using the Trajstat package (Wang et al., 2009b) for all four seasons (Figure 1). Although
226 cluster analysis revealed the predominance of continental transport in spring, fall, and winter
227 seasons, the air masses over the KCOG in summer mostly originated from the WNP. Since

spring is a transition of winds switching from westerlies to easterlies, Gosan is likely influenced by the long-range transport of dust, pollution, and sea-salt aerosols.

The vertical mixing of pollutants within the boundary layer height also plays an important role in controlling the strength of continental outflow alongside regional meteorology. For instance, the mixing height of air parcels from the HYSPLIT model is mostly confined to 1000 m in winter but somewhat increased towards spring and fall seasons (Figure S1). This vertical enhancement in the boundary layer height facilitates the transport of mineral dust particles from the arid and semiarid regions in East Asia along with urban pollutants to Gosan in spring and fall compared to winter. However, the strength of continental outflow somewhat depends on several factors, including source emissions, meteorology, and mixing height of air parcels.

Gosan is influenced by three types of air masses in spring (Figure 1a), from the Mongolian Desert (cluster 1: 15%), North China (cluster 2: 45%), and from the Yellow Sea (cluster 3: 40%). In contrast, the easterlies from the WNP in summer mostly influenced the composition of TSP over the KCOG. This inference is based on the cluster analysis for summer samples (Figure 1b), which showed four regimes, including transport from the Sea of Japan (cluster 1: 13%), WNP (cluster 2: 22%), South China Sea (cluster 3: 46%), and East China Sea (cluster 4: 19%). In contrast, cluster analysis revealed three major transport regimes from East Asia in fall and winter (Figure 1c-d). However, there are subtle differences that exist between winter and fall in terms of influence from nearby versus distant pollution sources. For instance, long-range transport of air masses from west Mongolia (cluster 1: 21%) and the Russian Far East (cluster 3: 14%) exerted a weak influence on the TSP sampled over Gosan in winter. Besides, we observed a somewhat larger impact of air masses from the North China Plain over Gosan (cluster 2: 64%) in winter. In contrast, Gosan is less influenced by air masses originating from the North China Plain, contributing ~28% (cluster 1) than those from Mongolia (cluster 2: 39%) and Russian Far East (cluster 3: 33%) in fall. Therefore, the impact of East Asian outflow is stronger in winter than in spring and fall.

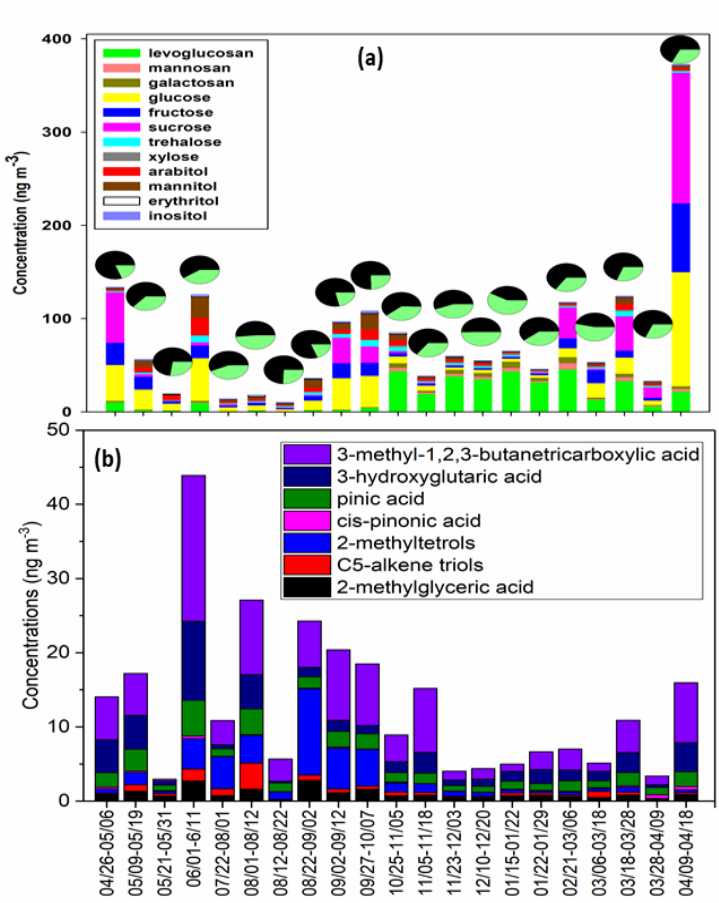

Figure 2. (a) Cumulative concentration levels of anhydrosugars, primary sugars, and sugar alcohols (i.e., represented by bars), and depicting the contributions of nonfossil (green color) and fossil (black color) organic carbon (i.e., pie charts), (b) Cumulative concentration levels of isoprene- and monoterpene SOA tracers in each TSP sample collected over Gosan.

3.2. Temporal and seasonal variability of sugars

The temporal/seasonal trends of sugar compounds over the KCOG provide useful information on the emission strengths of various sources in the East Asian outflow. All three anhydrosugars showed similar temporal and seasonal trends with higher concentrations in winter and fall than spring and summer (Figures 2a and S2). As levoglucosan and other two anhydrosugars (mannosan and galactosan) are the pyrolysis products of cellulose/hemicellulose, their higher concentrations along with an increase in nonfossil fraction of OC (Figure 2a; pie charts) in TSP from winter and fall revealed the impact of BB emissions. The MODIS satellite-based fire counts (Figure S1) together with cluster analysis in winter and fall (Figure 1) have revealed an influence of active BB emissions in the North China Plain, Mongolia, and Russian Far East. The temporal trends of glucose, fructose, and sucrose exhibited less variability throughout the sampling period; however, we observed a

slight increase in their concentration towards spring/summer (Figure 2a). Glucose and fructose have origins from leaf fragments and pollen species (Fu et al., 2012a). Sucrose is a potential tracer for airborne pollen (Fu et al., 2012a) and late spring/early summer is often regarded as a season of "pollen-allergies". Therefore, similar temporal trends of glucose and fructose with sucrose indicate their common source, pollens (Figure 2a). Since glucose, fructose, and sucrose showed moderately significant correlations (R^2 = 0.44-0.48, $p<0.01$) with levoglucosan in winter, it is somewhat possible that BB source emission could also influence the concentrations of these saccharides in this season (Haque et al., 2019; Fu et al., 2008).

BB also contributes to xylose and, hence, the temporal variability of xylose is mimicking that of anhydrosugars. Trehalose is a primary sugar and a useful tracer for organic carbon associated with soil dust particles (Fu et al., 2012a). The temporal variability of trehalose closely resembled that of fungal spore tracers (arabitol, mannitol, and erythritol), showing high concentrations in spring, summer, and fall seasons (Figures 2a and S2) (Zhu et al., 2015a; Fu et al., 2012a). The KCOG is under the influence of a large-scale advection of mineral dust from East Asia to the WNP during these three seasons (Tyagi et al., 2017; Huebert et al., 2003). The mineral dust transport from East Asia to the WNP can be traced by the high concentrations of non-sea-salt Ca^{2+} in the TSP samples from Gosan (Arimoto et al., 1996). Similar temporal trends of trehalose and nss-Ca^{2+}, particularly in spring samples (Figure S3), suggest that the abundance of OA specific to fungal spores over Gosan is likely associated with the Kosa (Asian dust) events.

The major sources of arabitol and mannitol are airborne fungal spores (Bauer et al., 2008), accompanying detritus from mature leaves (Pashynska et al., 2002). Heald and Spracklen (2009) reported that mannitol and arabitol are considerably associated with terrestrial biosphere activity. Inositol is largely derived from the developing leaves in summer (Pashynska et al., 2002) and BB in winter (Fu et al., 2010b). Zhu et al. (2015b) found similar seasonal behavior of inositol with those of other sugar alcohols with the predominance in summer, associated with microbial activities in local forests from Okinawa. Inositol showed a moderately significant correlation with levoglucosan (R^2 = 0.33, $p< 0.01$) in winter; however, there were no positive linear relationships between levoglucosan and other sugar alcohols, implying a partial emission of inositol from the BB during winter in Gosan aerosols. Therefore, the temporal variability of inositol differs from other sugar alcohols (Figure S2). The sources of sugar compounds are further discussed in section 3.4.

The seasonally averaged concentrations of all the anhydrosugars and xylose are higher in winter/fall than spring/summer (Figure 3a-d), possibly due to a greater influence of long-range transport from East Asia. In contrast, glucose, fructose, and sucrose peaked in spring but decreased in other seasons (Figure 3e-g), mainly because of the contribution of airborne pollen. Trehalose showed higher concentrations in fall and summer, followed by spring and winter (Figure 3h). Arabitol, mannitol, and erythritol showed higher concentrations in summer/fall than in winter and spring (Figure 3i-k). This seasonal trend is consistent with those of soil-derived fungal spores. This feature is consistent with earlier observations from a remote oceanic island in the WNP (Okinawa) during the impact of East Asian outflow (Zhu et al., 2015a). The seasonally averaged mass concentrations of inositol are highest in spring, followed by summer, fall, and winter (Figure 3l). Overall, the molecular compositions of anhydrosugars showed the predominance of levoglucosan followed by galactosan and mannosan (Figure S4**)**. Galactosan is more abundant in crop-residue burning emissions than mannosan (Engling et al., 2009; Sheesley et al., 2003). It is very much likely that the impact of crop-residue burning emissions in East Asia over Gosan is more prominent in winter/spring. Such high abundances of galactosan over mannosan were found in the North China Plain (Fu et al., 2008) and in the Indo-Gangetic Plain outflow sampled over the Bay of Bengal (Bikkina et al., 2019). Although the temporal variability of primary sugars in the TSP samples from Gosan showed a characteristic peak of glucose and sucrose (Figure 2a), the seasonally averaged distributions are different (Figure S4**)**. The molecular distributions of sugar alcohols are characterized by high loadings of arabitol and mannitol, followed by erythritol and inositol (Figure S4).

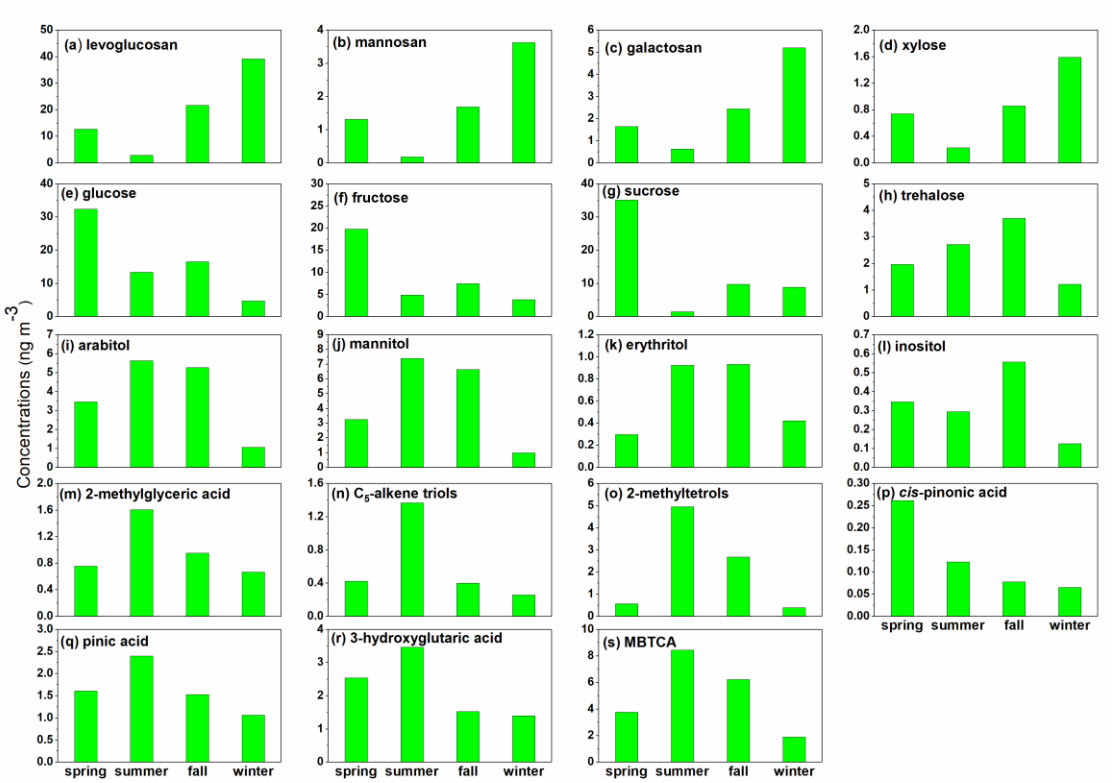

Figure 3. Seasonal variability of atmospheric levels of sugar compounds and BSOA tracers in TSP samples from Gosan during April 2013-April 2014.

3.3. Temporal and seasonal variability of BSOA tracers

We identified six isoprene-SOA tracers such as 2-methylglyceric acid (2-MGA), three C_5-alkene triols, and two 2-methyltetrols (2-methylthreitol and 2-methylerythritol) (2-MTs) in Gosan aerosol samples (Table 1). The sum of isoprene-SOA tracers ranged from 0.35 to 15.1 ng m^{-3} (avg. 3.69 ng m^{-3}) with the predominance of 2-MTs (avg. 2.09 ng m^{-3}). 2-MGA is the second most abundant isoprene-SOA tracer (avg. 0.99 ng m^{-3}), a high-generation product probably formed by further photooxidation of methacrolein and methacrylic acid. A similar molecular composition was observed over the North Pacific and California Coast (Fu et al., 2011). All the isoprene SOA tracers exhibited similar temporal variations with higher concentrations in the summer/spring months compared to autumn and winter (Figure 2b). Conversely, four monoterpene-SOA tracers, i.e., *cis*-pinonic acid, pinic acid, 3-hydroxyglutaric acid (3-HGA), and 3-methyl-1,2,3-butanetricarboxylic acid (MBTCA), were detected in Gosan samples (Table 1). Total concentrations of monoterpene-SOA tracers were found to be 1.65 to 35.5 ng m^{-3} (avg. 9.24 ng m^{-3}) with a high concentration of MBTCA (avg. 5.11 ng m^{-3}). All the monoterpene-SOA tracers showed similar temporal trends with high values in summer/spring periods than autumn/winter (Figure 2b). Nevertheless, *cis*-

pinonic acid was ascribed somewhat different temporal variability with other monoterpene-SOA tracers. It is likely that *cis*-pinonic acid might be further photo-oxidized to form MBTCA (Szmigielski et al., 2007).

The seasonal average of isoprene-SOA tracers showed high concentrations in summer, followed by spring/fall and winter (Figure 3m-o). One key feature of the data presented here is that two fall samples (KOS984; 2-12 September and KOS986; 27 September to 07 October) exhibited high concentrations for 2-MTs over Gosan (Figure 2b). We presumed that local vegetation might contribute significantly to the formation of 2-MTs as it is a first-generation product. Moreover, 2-MTs can be derived from the open ocean under low NO_x conditions (Hu et al., 2013). 3-HGA and pinic acid showed somewhat higher concentrations in summer/spring than fall/winter due to the growing vegetation (Figure 3q-r). *Cis*-pinonic acid was more abundant in spring compared to summer (Figure 3p) because of its photo-degradation, as discussed above. In contrast, MBTCA was dominant in summer/fall than spring/winter (Figure 3s). Here, the formation of MBTCA could be enhanced in fall during atmospheric transport from East Asia. The molecular distributions of isoprene-SOA tracers were characterized by a high loading of 2-MTs, followed by 2-MGA and C_5-alkene triols in all seasons (Figure S4). The Molecular composition of monoterpene-SOA tracers was dominated by MBTCA, followed by 3-HGA, pinic acid, and *cis*-pinonic acid in all seasons (Figure S4). Overall, BSOA tracers were found to be most abundant in summer, followed by fall, spring, and winter (Table 1). Interestingly, it is likely that secondary OA undergoes much faster cycling than the primary sugar compounds, considering the feasibility of photooxidation. This would mean a slight underestimation of BSOA over the KCOG in the East Asian outflow and, hence, their atmospheric abundances over Gosan reflect a lower limit.

Kang et al. (2018b) reported that monoterpene-SOA tracers were more abundant than isoprene-SOA tracers in spring-summer over the East China Sea, which is consistent with this study. Although the mass budget calculations showed that isoprene and monoterpenes are largely emitted by terrestrial plants; however, the open ocean can also contribute to isoprene and monoterpenes significantly (Conte et al., 2020; Shaw et al., 2010; Broadgate et al., 1997). Air mass back trajectory and cluster analysis (Figure 1) implied that air masses mostly originated from the ocean during summer. This means the open ocean significantly contributed to isoprene-SOA production. However, terrestrial sources from the continent also substantially enhanced the formation of BSOA. For example, one sample (KOS: 979; 1-11

June 2013) during summer showed the highest loading of BSOA tracers (Figure 2b) when air masses are transported from the continent (Zhang et al., 2016).

Figure 4. Multiple linear regression (MLR) analysis of airborne sugar compounds in TSP collected over Gosan.

3.4. Source apportionment- regression analysis and diagnostic ratios

Anhydrosugars strongly correlated with xylose (Figure 4), suggesting their common source as BB emission in East Asia. Fu et al. (2012a) analyzed pollen from different tree species (*e.g.*, White birch, Chinese willow, Peking willow, Sugi, Hinoki), which are enriched in sucrose (182-37,300 μg g^{-1}), glucose (378-3601 μg g^{-1}) and fructose (162-1813 μg g^{-1}). In our samples, sucrose strongly correlated with glucose and fructose (Figure 4), suggesting their origin from plant-derived airborne pollen. Likewise, a strong correlation was found between arabitol and mannitol, indicating a mutual origin from a similar type of fungal spores (Zhu et al., 2015a; Fu et al., 2012a; Bauer et al., 2008; Yttri et al., 2007). Bauer et al. (2008) ascribed

weak correlations between arabitol and mannitol to the diverse nature of ambient fungal spores. Furthermore, both sugar alcohols correlated well with trehalose, a tracer for soil organic carbon (Fu et al., 2012a). This observation suggests their common origin from soil organic matter associated with fungal spores. Erythritol also originates from fungal spores; however, its abundance is affected by the atmospheric aging process. Kessler et al. (2010) reported that erythritol is degraded during long-range transport in 12.7 days. Consequently, arabitol and mannitol were moderately correlated with erythritol in the Gosan samples due to the degradation of latter sugar alcohol in the East Asian outflow.

The linear relationship of levoglucosan (*Lev*) with mannosan (*Man*), galactosan (*Gal*), and nss-K^+ provide useful information on the type of BB emissions (hardwood, softwood, or crop-residue). Ratios of *Lev*/*Man* and *Lev*/(*Man* + *Gal*) can be useful to distinguish BB and coal combustion contributions. The average ratios of *Lev*/*Man* (15.1 ± 6.76) and *Lev*/(*Man* + *Gal*) (4.27 ± 1.23) in Gosan aerosols are much closer to those from wood burning and coal combustion sources emissions, respectively (Yan et al., 2018). It reveals that *Lev* could originate from both biomass and coal burning source emissions, which is consistent with the linear relationship between *Lev*-C and fossil-/nonfossil carbon fraction (section 3.7). Furthermore, different types of biomass are characterized by distinct *Lev/Man* ratios. For instance, *Lev/Man* ratios from the softwood burning emissions (3-10) differ from those of hardwood (15-25) and crop-residues (>40) (Singh et al., 2017; Schmidl et al., 2008a, b; Fu et al., 2008; Engling et al., 2006, 2009; Fine et al., 2001, 2004). We found the *Lev/Man* ratios (Table 2) over the KCOG overlap between seasons and somewhat close to that of hardwood burning emissions in northern China, Mongolia, and the Russian Far East, as corroborated by the backward air mass trajectories and MODIS fire counts (Figures 1 and S1). Besides, *Lev*/K^+ and *Man/Gal* ratios in summer differ from those of other seasons (Table 2). Cheng et al. (2013) have apportioned qualitatively the source contributions of anhydrosugars over a receptor site based on the comparison of *Lev*/K^+ and *Lev/Man* ratios in aerosols to those from various sources profiles compiled from the literature. This approach of using the mass ratios of *Lev/Man* and *Lev*/K^+ has been proven useful for deciphering the difference in BB-derived OA (Bikkina et al., 2019).

Here, we adopted this methodology to ascertain the likely contributing sources of anhydrosugars, which are BB tracers from different seasons (Figure 5). This source apportionment relies on the fact that *Lev*/K^+ from the softwood burning (10-1000) is higher than hardwood (1-100) (Fine et al., 2004). In contrast, *Lev*/*Man* ratios for softwood are lower than those of hardwood burning (10-100) (Fine et al., 2004). Likewise, the *Lev/Man* and

Lev/K^+ ratios from grasses and crop-residues are 10-100 and 0.01-1.0, respectively (Bikkina et al., 2019). On a similar note, the *Lev*/K^+ ratios from the burning of pine needles (0.1-1.0) somewhat overlap with hardwood burning emissions but are characterized by distinct *Lev/Man* ratios (Bikkina et al., 2019). The burning of dead leaves (duff) showed higher *Lev*/K^+ than pine needles and grasses, but their *Lev/Man* is on the lower side than the former biomass type and the softwood burning emissions. However, *Lev* is more susceptible to degradation by photooxidation with OH radicals during atmospheric transport (half-life: <2.2 days) (Hennigan et al., 2010) and, this would cause lower abundances of this anhydrosugar. Hence, the hardwood *Lev*/K^+ ratios could slightly shift downwards. Therefore, caution is required while interpreting the ambient data from a receptor site (Bikkina et al., 2019). Overlapping the seasonal data on this scatter plot of *Lev*/K^+ versus *Lev/Man* (Figure 5) clearly revealed a mixed contribution of burning of hardwood and crop-residue in the East Asian outflow. It should be noted that the photooxidation process during atmospheric transport is also applicable for low concentrations and poor correlations of other primary saccharides.

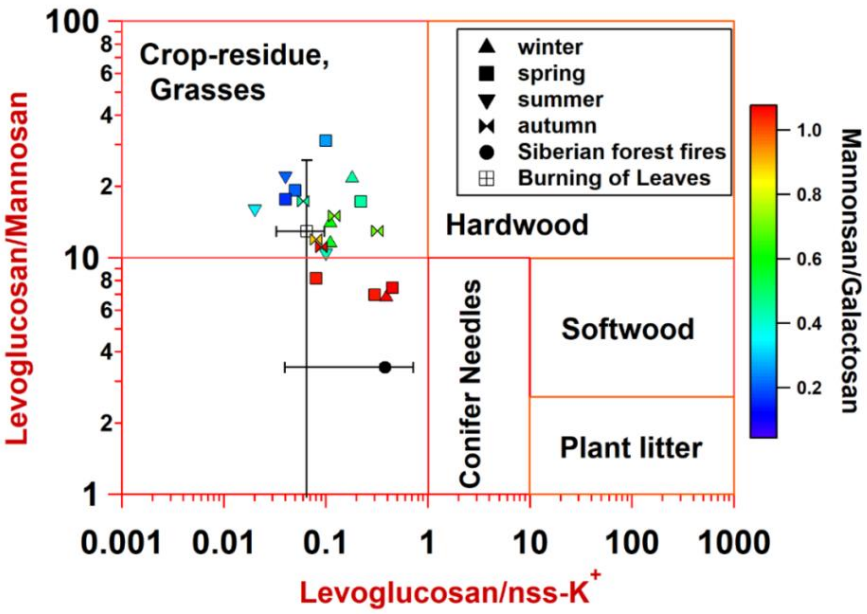

Figure 5. Scatter plot of levoglucosan/K^+ versus levoglucosan/mannosan ratios in TSP collected over Gosan during April 2013-April 2014. The data for Siberian forest fires and burning leaves were adopted from Sullivan et al. (2008).

The correlation coefficients and diagnostic ratios of BSOA tracers specify their source origin or formation pathway. Nevertheless, atmospheric stability or reactivity of BSOA tracers through the photooxidation during long-range transport may bias the correlation coefficients in Gosan aerosols. 2-MGA showed significant correlation with 2-MTs ($r = 0.79$, $p<0.01$) and C_5-alkene triols ($r = 0.50$, $p<0.05$) (Figure 6a-b), suggesting their similar formation pathway or common sources of isoprene SOA tracers. However, a poor correlation coefficient between 2-MTs and C_5-alkene triols ($r = 0.33$, $p = 0.13$) (Figure 6c) indicates their different formation process over the Gosan atmosphere. Wang et al. (2005) documented that polyols are formed from isoprene through diepoxy derivatives, which further convert into 2-MTs by acid-catalyzed hydrolysis. On the other hand, C_5-alkene triols are produced from the precursor of hydroxyperoxy radicals that are initially derived from isoprene through rearrangement reactions (Surratt et al., 2006). It can be noted that the formation mechanisms of 2-MGA and 2-MTs are different while depending on the NO_x concentrations (Surratt et al., 2010). Thus, the ratio of 2-MGA/2-MTs attributes to the influence of NO_x on isoprene SOA formation. We found a low ratio of 2-MGA/2-MTs (0.67) (Figure S5a, Table 2) in summer, implying enhancement of 2-MTs formation over the open ocean due to the low-NO_x environment in the ocean atmosphere. On the contrary, 2-MGA/2-MTs ratios for other seasons were >1.0 (Figure S5a, Table 2), indicating an elevated formation of 2-MGA through continental high NO_x condition, which is consistent with air masses back trajectory.

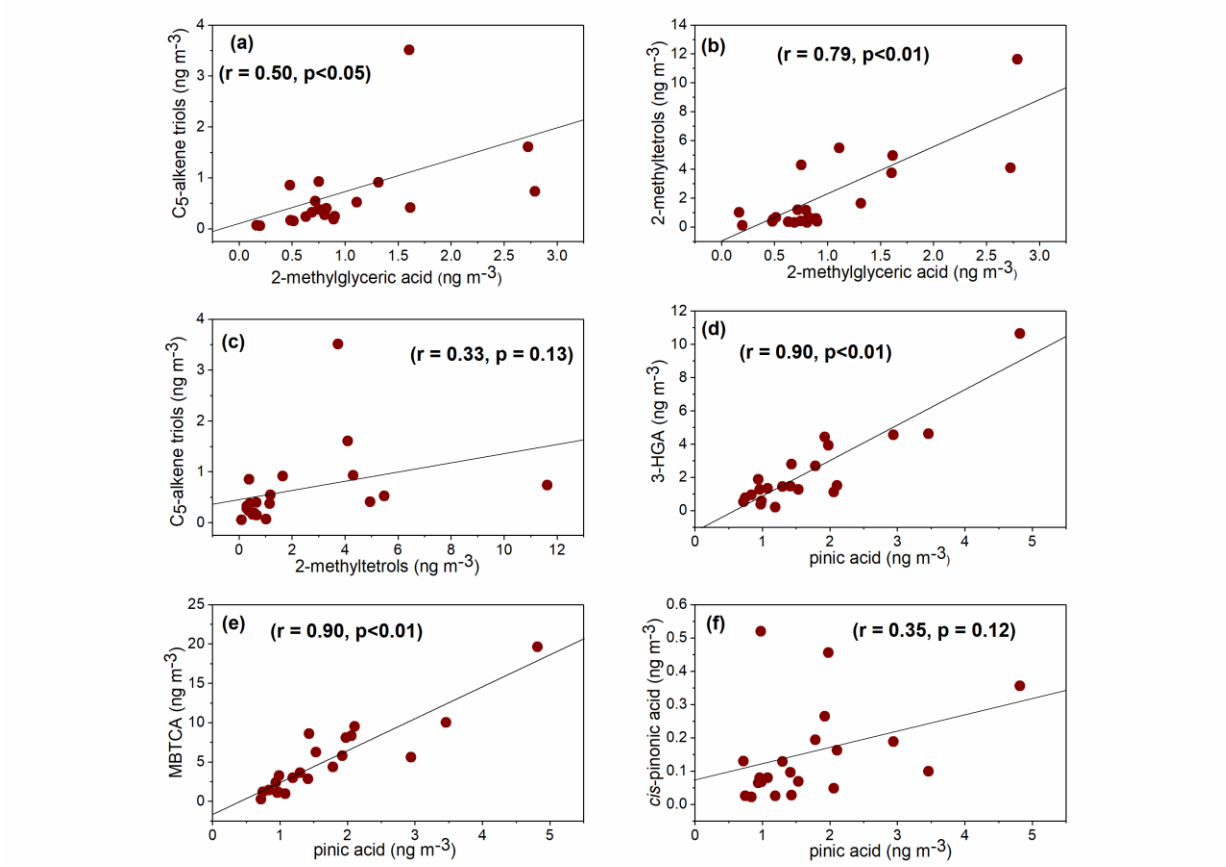

Figure 6. Pearson linear correlation coefficient analysis of BSOA tracers in Gosan TSP aerosols during April 2013-April 2014.

Cis-pinonic acid showed a weak correlation with pinic acid (r = 0.35, p = 0.12) (Figure 6f), suggesting that different atmospheric reactivity of cis-pinonic/pinic acids during transport would cause such poor correlation. In contrast, pinic acid exhibited a strong positive linear correlation with 3-HGA (r = 0.90, p<0.01) and MBTCA (r 0.90, p<0.01) (Figure 6d-e), implying their similar sources. It should be noted that the formation processes of pinic acid, 3-HGA, and MBTCA are different because pinic acid is a first-generation product, and 3-HGA and MBTCA are high-generation products (Claeys et al., 2007; Müller et al., 2012; Szmigielski et al., 2007). The ratio of *cis*-pinonic acid + pinic acid to MBTCA (P/M) is used to evaluate the aging of monoterpene SOA.

A low P/M ratio suggests the transformation of *cis*-pinonic and pinic acids to MBTCA and thus relatively aged monoterpene-SOA, whereas a high ratio reflects relatively fresh monoterpene-SOA (Gómez-González et al., 2012; Ding et al., 2014). Gómez-González et al. (2012) reported aged monoterpene-SOA (P/M = 0.84) from a Belgian forest site while fresh chamber-produced α-pinene-SOA tracers showed P/M ratios of 1.51 to 3.21 (Offenberg

et al., 2007). The average ratio of P/M in this study showed 0.62 with the low value in summer (Figure S5b, Table 2), which is lower than those of Guangzhou (fresh monoterpene-SOA; 28.9) while the air masses originated from southern China (Ding et al., 2014). This observation indicates that monoterpenes SOA have undergone substantial aging during transport to Gosan, particularly in summer when extensive photochemical oxidation occurred due to the high temperature and intense solar radiation.

3.5. Source apportionment - Positive Matrix Factorization (PMF) analysis

We used the positive matrix factorization (PMF) analysis of airborne sugar compounds and BSOA tracers to assess their sources over Gosan. Five-factor profiles were chosen that could best explain the data (Figure 7). In factor 1, we found higher loadings of sucrose (88%), fructose (57%), and glucose (40%). Sucrose is a well-known tracer for airborne pollen as these types of biogenic sources also contain significant levels of glucose and fructose; we attribute this factor to contribution from "pollen". Likewise, factor 2 has higher loadings of C_5-alkene triols (54%), 2-MGA (38%), *cis*-pinonic acid (34%), pinic acid (33%), and 3-HGA (33%). These SOA tracers are formed by the photochemical oxidation of BVOCs (e.g., isoprene and monoterpene), which are emitted from terrestrial vegetation and oceanic phytoplankton. Therefore, we attribute factor 2 to biogenic secondary oxidation products. Factor 3 was abundantly loaded by non-sea-salt fraction of calcium (nss-Ca^{2+}), implying that the component is associated with soil dust as nss-Ca^{2+} is a specific tracer of Earth surface soil (Athanasopoulou et al., 2010; Brahney et al., 2013). It should be noted that significant loadings were also observed for trehalose (39%), glucose (35%), and fructose (35%) in factor 3, indicating their association with soil microbes.

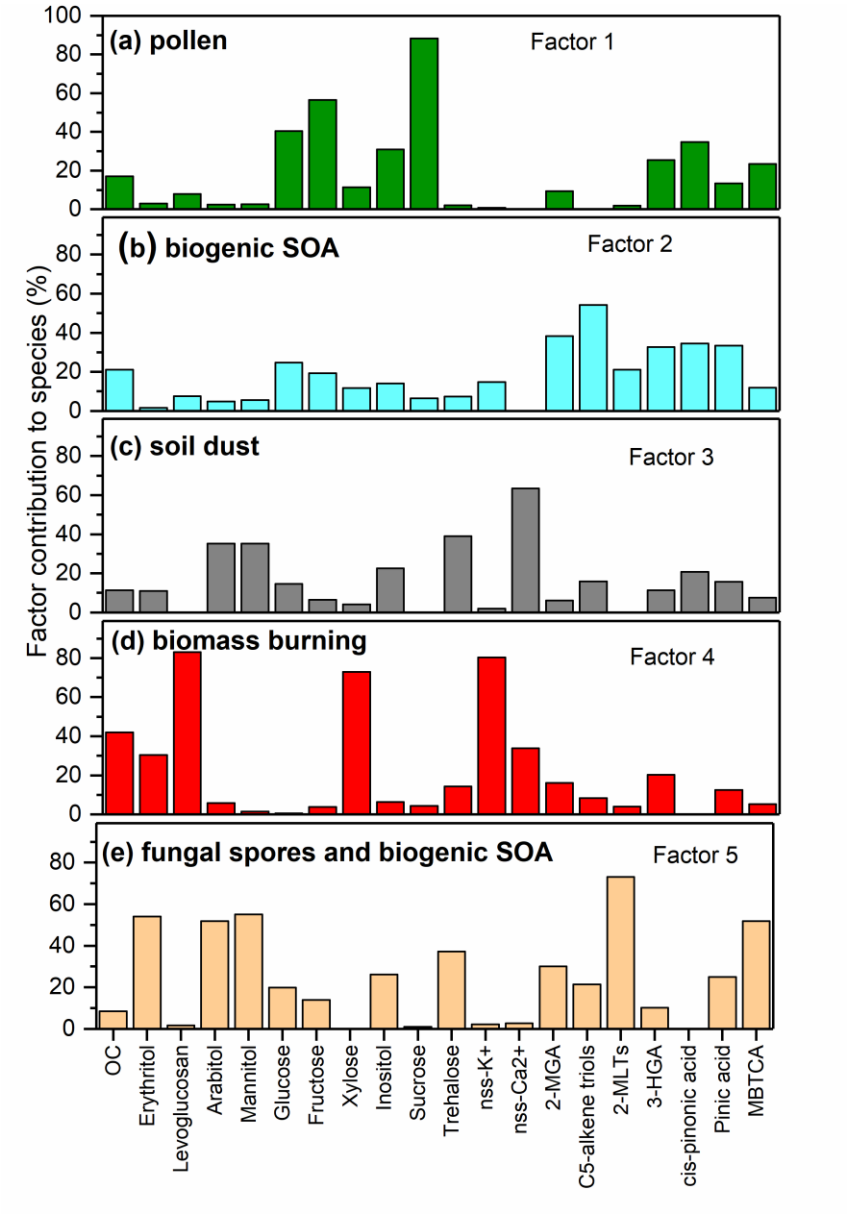

535

536 **Figure 7.** Positive Matrix Factorization (PMF)- based Source profiles resolved for the
537 measured primary saccharides in TSP collected over Gosan during April 2013-April 2014.

538

539 We found high loadings of levoglucosan (83%), nss-K^+ (80%), and xylose (73%) in
540 factor 4. Such high contributions of levoglucosan and K^+ (hemicellulose/cellulose pyrolysis
541 tracers) and xylose (wood sugar) are typical of wood burning emissions. We, therefore,
542 ascribe this factor to the influence of BB emissions in East Asia over Gosan. Factor 5 is
543 dominated by 2-MTs (73%), MBTCA (53%), mannitol (55%), erythritol (54%), and arabitol
544 (52%). 2-MTs and MBTCA are BSOA tracers, which are produced by the photooxidation of
545 isoprene and monoterpene, respectively. In contrast, arabitol, mannitol, and erythritol are
546 typical tracers of airborne fungal spores (Lewis and Smith, 1967; Bauer et al., 2008). Thus,

547 factor 5 is associated with mixed sources of 'fungal spores' and 'biogenic secondary
548 oxidation products'. PMF results were further utilized to calculate the relative contributions
549 from various sources to OC over Gosan (Figure S6). BB was the dominant source of OC over
550 Gosan (41.9%), followed by BSOA (21.1%), pollen (17.1%), and soil dust (11.4%).

551 **3.6. Relative abundances in WSOC and OC**

552 Levoglucosan is the most abundant anhydrosugar, contributing 0.05-1.54% of WSOC and
553 0.03-1.02% of OC. Likewise, sucrose, glucose, and fructose were more abundant primary
554 sugars, contributing 0.01-2.83%, 0.03-1.22%, and 0.02-0.74% of WSOC, respectively.
555 Contributions of the three primary sugars varied from 0.05% to 3.41% of OC. Arabitol and
556 mannitol are the most abundant sugar alcohols, whose contribution to WSOC and OC ranged
557 from 0.02% to 0.93% and 0.01% to 0.85%, respectively. Figure 8 depicts the contribution of
558 sugar compounds to WSOC and OC in TSP collected over Gosan during the study period.
559 We also compared the atmospheric abundances of sugar compounds from Gosan with the
560 literature data (Table 3). This comparison revealed the less influence of BB tracer compounds
561 (i.e., anhydrosugar levels) over Gosan, a factor of 5-10 times lower than those reported for
562 the BB-influenced source regions in China and East Asia (Fu et al., 2012b; Kang et al.,
563 2018a; Wang and Kawamura, 2005; Wang et al., 2012). However, the levels of anhydrosugar
564 over Gosan are higher than those observed over the remote Canadian High Arctic site (Fu et
565 al., 2009a). In contrast, Gosan is characterized by high concentrations of primary sugars
566 compared to other remote sampling sites in Table 3. This is because of the overwhelming
567 contribution of primary sugars associated with soil dust particles over Gosan during the East
568 Asian outflow. Such high loadings of primary sugars were observed from other remote island
569 receptor sites in the WNP (Okinawa) during the spring season (Zhu et al., 2015a). Likewise,
570 the concentrations of sugar alcohols from Gosan are similar to those from other receptor sites
571 influenced by the East Asian outflow (Verma et al., 2018; Zhu et al., 2015a).

572

573

574

575

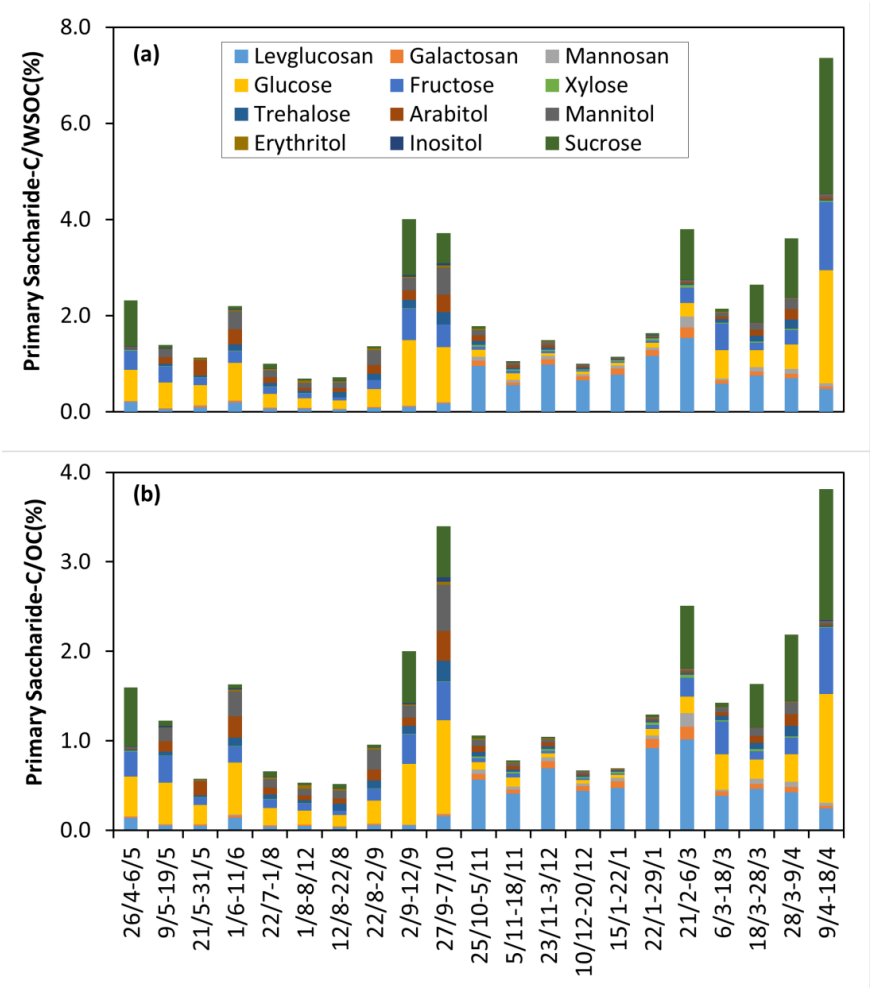

Figure 8. Contribution of primary saccharide-C in (a) WSOC(%) and (b) OC(%) in TSP collected over Gosan during April 2013-April 2014.

Contributions of isoprene-SOA tracers to ambient OC (0.01-0.40%, avg. 0.09%) and WSOC (0.02-0.57%, 0.13%) were lower than monoterpene-derived SOA (0.04-0.63%, 0.23% for OC and 0.06-0.82%, 0.33% for WSOC). The contributions of isoprene oxidation products to OC and WSOC were found to be highest in summer (0.23% and 0.32%, respectively), followed by fall (0.09% and 0.13%), spring (0.04% and 0.06%), and winter (0.02% and 0.03%). Likewise, the contributions of monoterpene-SOA products to aerosol OC and WSOC exhibited highest value in summer (0.40% and 0.55%, respectively), followed by fall (0.24% and 0.35%), spring (0.18% and 0.27%), and winter (0.10% and 0.14%). We found that the contribution of BSOA products to carbonaceous components was twice in summer (Figure 9, Table 2). This means SOA formation was occurred in summer to a greater extent due to the intensive BVOCs emission with key factors of meteorological parameters

591 (higher temperature and radiation), i.e., higher concentrations of ozone, and other oxidizing
592 agents (NO_x, OH, etc.).

593

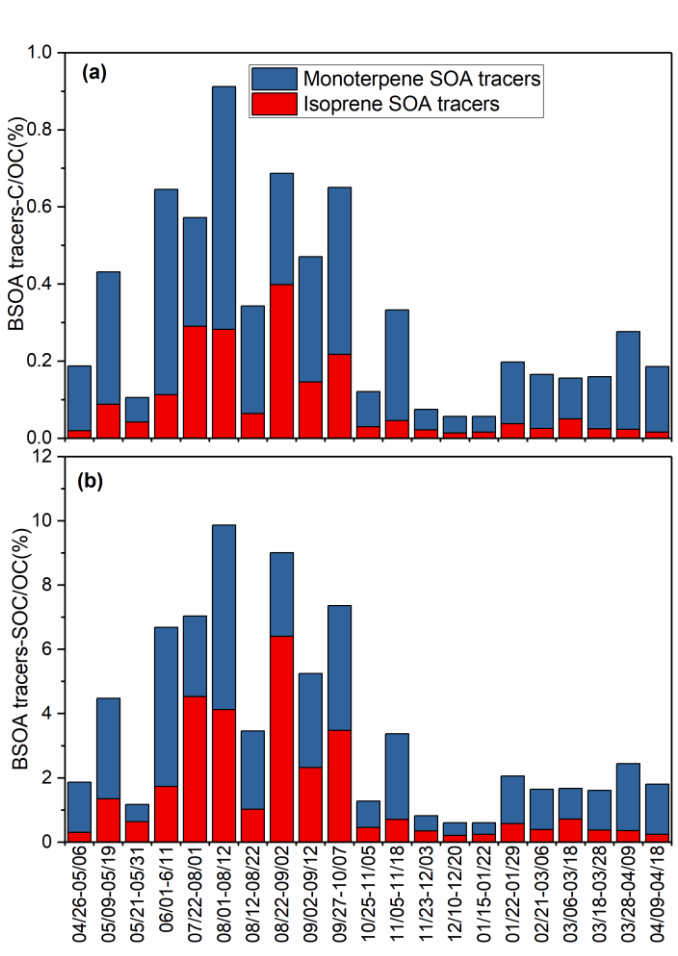

594

595 **Figure 9.** Contribution of (a) isoprene- and monoterpene SOA tracers-C in ambient OC(%)
596 and (b) isoprene- and monoterpene SOA tracers-SOC in ambient OC(%) in Gosan aerosol
597 samples during April 2013-April 2014.

598

599 We estimated secondary organic carbon (SOC) derived from isoprene and
600 monoterpenes, using the measured values of BSOA tracers and following the SOA tracer-
601 based method first proposed by Kleindienst et al. (2007). A summary of the estimated SOC is
602 provided in Table 2. The contribution of isoprene to SOC was calculated 2.26 to 97.4 ngC m^{-3}
603 (avg. 23.7 ngC m^{-3}), accounting for 1.45% of OC and 35.5% of total BSOC with the
604 predominance in summer (3.56% and 46.6% for OC and SOC, respectively). The estimation
605 of monoterpene SOA to SOC (avg. 40.1 ngC m^{-3}) was observed around two times higher than
606 isoprene (Table 2). Interestingly, the contribution of monoterpene-derived SOC to ambient

607 OC (3.65%) was dominant in summer, but monoterpene SOC to total SOC (72.1%) was most
608 abundant in spring (Figure 9b). The seasonal distributions of biogenic SOC (Table 2) implied
609 that a substantial amount of SOC was formed from monoterpenes in spring. The estimated
610 biogenic SOC at the KCOG is almost one order of magnitude lower than those from other
611 continental sites in China urban areas (e.g., Pearl River Delta: 446 ngC m^{-3}) (Ding et al.,
612 2012). However, the estimated biogenic SOC load from the KCOG is much higher than that
613 reported from a remote site in the Canadian High Arctic (Alert: 9.4 ngC m^{-3}) (Fu et al.,
614 2009b) and comparable with over the East China Sea (Kang et al., 2018b).
615 It should be noted that concentrations of SOA tracers cannot always provide the
616 actual contribution of the biogenic source to ambient organic aerosol mass. For example,
617 loadings of monoterpene-SOA tracers were lower in sample KOS999 (28 March - 9 April
618 2014) (3.02 ng m^{-3}) compared to sample KOS1000 (9 - 18 April 2014) (14.4 ng m^{-3}), whereas
619 the estimated contribution of SOC to ambient OC showed an opposite trend (KOS999:
620 2.08%; KOS1000: 1.56%). This result demonstrates that the estimation of SOC is an
621 important factor in evaluating the contribution of BSOA to organic aerosol mass. We
622 calculated biogenic OC using radiocarbon (^{14}C) data following the method proposed by
623 Szidat et al. (2006). Biogenic OC showed poor correlation with biogenic SOC ($r = 0.36$, $p = 0.09$) but significant linear relationship with primary sugars (i.e., glucose, fructose and
624 0.09) but significant linear relationship with primary sugars (i.e., glucose, fructose and
625 sucrose) ($r = 0.54$, $p<0.5$), suggesting that primary bioaerosols from plant-derived airborne
626 pollen dictate on biogenic OC over Gosan.

627 **3.7. Significance of fossil fuel as a source for levoglucosan**

628 The ambient levoglucosan (*Lev*) levels showed a significant linear relationship with the
629 OC_{fossil}, suggesting the fossil source contribution of this molecular marker (Figure 10a).
630 However, such a significant correlation was not evident between OC_{fossil} and other major
631 sugar compounds. Until recently, *Lev* has been thought to originate primarily from the
632 hemicellulose/cellulose pyrolysis of vegetation and, hence, can be employed as a powerful
633 tracer for biomass smoke particles (Fraser and Lakshmanan, 2000; Simoneit et al., 1999).
634 Nevertheless, residential coals (*e.g.,* lignite and bituminous coal) have been shown to contain
635 high concentrations of '*Lev*' but also emit traces of *Man and Gal* (Kourtchev et al., 2011;
636 Fabbri et al., 2008). Recently, Yan et al. (2018) found a significant linear relationship
637 between the ^{14}C-based fossil fraction of WSOC and *Lev-C* in the aerosols generated from
638 coal combustion and the ambient aerosol samples. Therefore, the prevailing linear
639 relationship between OC_{fossil} and *Lev*-C in Gosan samples (Figure 10a) is likely due to a
640 common source contribution from coal combustion in East Asia.

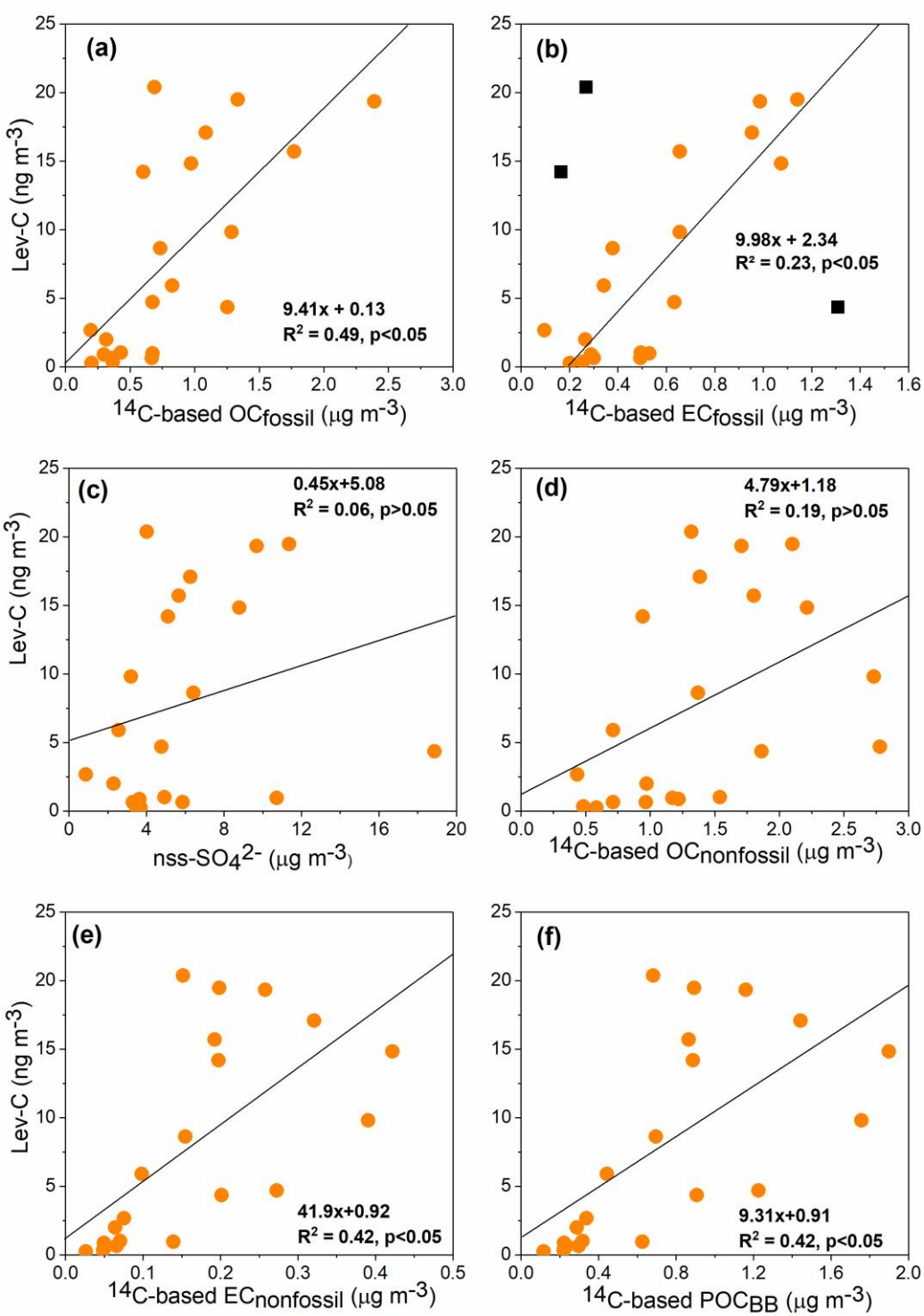

641

642 **Figure 10.** Linear regression analysis between levoglucosan in terms of their carbon content
643 (*Lev*-C) and ^{14}C-based mass concentrations of (a) organic carbon and (b) elemental carbon of
644 fossil origin (OC_{fossil} and EC_{fossil}, respectively), (c) nss-SO_4^{2-}, (d) nonfossil derived organic
645 carbon ($OC_{nonfossil}$), (e) nonfossil derived elemental carbon ($EC_{nonfossil}$), and (f) biomass
646 burning derived primary OC (POC_{BB}) in TSP collected over Gosan during April 2013-April
647 2014. In panel (b), the squares represent three outliers (i.e., samples with rather high and low
648 *Lev*/EC ratios; please see text for more details).

649 The slope of the linear regression between *Lev-C* and OC_{fossil} (0.0094; Figure 10a) is
650 higher than those documented for the coal combustion source in China (~0.004±0.007) (Yan
651 et al., 2018). Moreover, *Lev-C* moderately correlated with the EC_{fossil} with the regression
652 slope (~0.01) in Gosan samples (Figure 10b), being comparable to that observed for the coal
653 combustion in China (0.044±0.076) (Yan et al., 2018). It should be noted that excluding the
654 three outliers as shown in Figure 10b (black square), *Lev-C* showed a stronger correlation
655 with EC_{fossil} ($R^2 = 0.74$, $p < 0.05$). Of these, two outliers in winter (KOS995: 22-29 January
656 2014; KOS996: 21 February - 3 March 2014) have higher *Lev*-C levels over that of EC_{fossil},
657 when air mass trajectories showed the impact of BB emissions in the North China Plain. In
658 contrast, the third outlier in summer (KOS979: 1-11 Jun'2013) has a lower *Lev*-C/EC_{fossil},
659 while air parcels transported from nearby cities in China, Korea, and Japan, thus, have more
660 contribution from vehicular emissions. Overall, both the regression slopes are, thus, the
661 representative nature of *Lev*-C/OC_{fossil} and *Lev*-C/EC_{fossil} in the East Asian outflow. *Lev*-C and
662 nss-SO_4^{2-} exhibited a poor correlation (Figure 10c), although both were transported from East
663 Asia.

664 *Lev*-C exhibited a rather weak correlation with $OC_{nonfossil}$ ($R^2 = 0.19$) than that with
665 $EC_{nonfossil}$ ($R^2 = 0.42$) over Gosan during the study period **(**Figure 10d-e**)**. This could be likely
666 because $OC_{nonfossil}$ has contributions from the BB and the secondary formation process or the
667 primary biogenic sources. The contribution of primary OC generated from BB (POC_{BB}) to
668 $OC_{nonfossil}$ was taken from Zhang et al. (2016). In their study, the ^{14}C-based $EC_{nonfossil}$ levels
669 were scaled by a factor to constrain the POC_{BB} (Zhang et al., 2016). Here the conversion
670 factor is '4.5' (range: 3-10), which is a median value representing the primary OC/EC ratio
671 from BB emissions ($(POC/EC)_{BB}$).

672 $$POC_{BB} = EC_{nonfossil} \times (POC/EC)_{BB} \quad (7)$$

673 *Lev*-C showed a somewhat improved linear correlation with POC_{BB} than with the $OC_{nonfossil}$
674 (Figure 10f). It is apparent from Figure 10 that the regression slopes are comparable,
675 indicating their contribution to *Lev* from both coal combustion and BB emissions over Gosan.
676 The prevailing weak linear relationship (moderate correlation) of *Lev* with nonfossil and
677 fossil carbon fractions is likely being the result of photo-degradation of *Lev* during
678 atmospheric transport. This result would mean that the higher atmospheric abundance of *Lev*
679 and its pronounced linear relationships with the nonfossil and fossil carbon fractions implies
680 a much stronger impact of both source emissions in East Asia during the continental outflow
681 in winter and spring.

Overall, we present a new finding on the contribution of coal combustion sources in East Asia in controlling the atmospheric levels of *Lev* apart from the traditional biomass/biofuel burning emissions. This is based on the prevailing linear relationship between the radiocarbon based nonfossil-EC and *Lev* in the year-round TSP samples collected from the KCOG site in Jeju Island. The Gosan supersite is the best location to understand how the chemical composition of source-emissions from East Asia affects the outflow regions in winter and spring. Recent studies have highlighted the potential contribution of *Lev* from residential coal combustion in China (Yan et al., 2018), with estimated annual emission of ~2.2 Gg of *Lev* from domestic coal combustion (Wu et al., 2021). Given this background information, the prevailing significant linear relationship between *Lev* and nonfossil-EC (P-value < 0.05) over the KCOG clearly emphasizes the need for reconsideration of the previous assessments on the impact of BB in East Asian outflow to the WNP. Additionally, this dataset is further compared with the molecular distributions and relative abundances of organic tracers in the TSP samples collected over Gosan during 2001, a decade ago (Fu et al., 2012). This comparison allows us to better understand the regional changes in the emission sources (*e.g.*, fugitive dust, BB, and fossil-fuel combustion) on a decadal basis.

4. Conclusions

We investigated seasonal variations of primary organic components such as anhydrosugars, primary sugars, and sugar alcohols and biogenic secondary organic aerosol (BSOA) tracers (isoprene- and monoterpene-derived SOA products) in ambient aerosols from Gosan, Jeju Island. Among the detected sugar compounds, levoglucosan was dominant in winter/fall, whereas glucose and sucrose were more abundant in spring/summer. The seasonal trends documented that BB impact is more significant in winter/fall and the primary bioaerosol particles are important in spring/summer. Diagnostic ratios of levoglucosan, galactosan, and mannosan reflect that emissions from BB are mostly dominated by hardwood. The significant linear relationship of sucrose with glucose and fructose suggests their origin from airborne pollen. On a similar note, trehalose showed a significant positive correlation with arabitol, mannitol, and erythritol, implying their contribution from airborne fungal spores and soil microbes over the KCOG.

Distributions of biogenic SOA tracers were characterized by a predominance of monoterpene- than isoprene-derived oxidation products in Gosan aerosols. The BSOA tracers were formed in summer to a greater extent, followed by fall/spring and then winter. The low ratio of *cis*-pinonic acid + pinic acid to MBTCA (P/M) demonstrated that monoterpene SOA

was relatively aged over Gosan aerosols. The estimated secondary organic carbon (SOC) with the predominance in summer shows that substantial SOA formation occurred in summer due to favorable meteorological conditions. The backward air mass trajectories and source apportionment studies entirely demonstrated that BB and biogenic SOA contribution significantly dominate the ambient OA mass over KCOG. Interestingly, levoglucosan-*C* exhibited a significant positive correlation with nonfossil and fossil organic carbon fractions, along with the comparable regression slopes. This result reveals that BB and coal (lignite) combustion both are the prominent source for levoglucosan in the East Asian outflow.

Although there is some evidence that levoglucosan could originate from the combustion of brown coals (*e.g.*, lignite) in China; however, our observations are from the KCOG (receptor site) also hinted at the fossil source contribution of this molecular marker in the regional influx of the East Asian outflow. Therefore, attribution of ambient levoglucosan levels over the WNP to the impact of BB emission may cause large uncertainty.

Data availability

The data used in this paper are available upon request from the corresponding author.

Author contributions

KK and YLZ designed the research. ML collected the aerosol samples. MMH and SB performed the analysis of aerosol samples. MMH wrote the paper under the guidance of YLZ and KK. All authors were actively involved in the discussion of the paper.

Competing interests

The authors declare that they have no conflict of interest.

Acknowledgments

We acknowledge the financial supports of the Japan Society for the Promotion of Science (JSPS) through Grant-in-Aid No. 24221001 and the National Natural Science Foundation of China (Grant No 41977305).

References

Arimoto, R., Duce, R. A., Savoie, D. L., Prospero, J. M., Talbot, R., Cullen, J. D., Tomza, U., Lewis, N. F., and Ray, B. J.: Relationships among aerosol constituents from Asia and the North Pacific during PEM-West A, J. Geophys. Res. Atmos., 101, 2011-2023, https://doi.org/10.1029/95JD01071, 1996.

Athanasopoulou, E., Tombrou, M., Russell, A. G., Karanasiou, A., Eleftheriadis, K., and Dandou, A.: Implementation of road and soil dust emission parameterizations in the aerosol model CAMx: Applications over the greater Athens urban area affected by natural sources, J. Geophys. Res., 115, D17301, https://doi.org/10.1029/2009JD013207, 2010.

751 Bauer, H., Claeys, M., Vermeylen, R., Schueller, E., Weinke, G., Berger, A., and Puxbaum,
752 H.: Arabitol and mannitol as tracers for the quantification of airborne fungal spores,
753 Atmos. Environ., 42, 588–593, 2008.
754 Bikkina, S., Haque, M. M., Sarin, M., and Kawamura, K.: Tracing the relative significance of
755 primary versus secondary organic aerosols from biomass burning plumes over coastal
756 ocean using sugar compounds and stable carbon isotopes, ACS Earth Space Chem., 3,
757 1471-1484, https://doi.org/10.1021/acsearthspacechem.9b00140, 2019.
758 Bikkina, S., Kawamura, K., Sakamoto, Y., and Hirokawa, J: Low molecular weight
759 dicarboxylic acids, oxocarboxylic acids and α-dicarbonyls as ozonolysis products of
760 isoprene: Implication for the gaseous-phase formation of secondary organic aerosols, Sci.
761 Total Environ., 769, 144472, https://doi.org/10.1016/j.scitotenv.2020.144472, 2021.
762 Brahney, J., Ballantyne, A. P., Sievers, C., and Neff, J. C.: Increasing Ca^{2+} deposition in the
763 western US: The role of mineral aerosols, Aeolian Res., 10, 77–87, 2013.
764 Broadgate, W. J., Liss, P. S., and Penkett, S. A.: Seasonal emissions of isoprene and other
765 reactive hydrocarbon gases from the ocean, Geophys. Res. Lett., 24, 2675-2678,
766 https://doi.org/10.1029/97GL02736, 1997.
767 Cheng, Y., Engling, G., He, K.-B., Duan, F.-K., Ma, Y.-L., Du, Z.-Y., Liu, J.-M., Zheng, M.,
768 and Weber, R. J.: Biomass burning contribution to Beijing aerosol, Atmos. Chem. Phys.,
769 13, 7765–7781, 2013.
770 Claeys, M., Graham, B., Vas, G., Wang, W., Vermeylen, R., Pashynska, V., Cafmeyer, J.,
771 Guyon, P., Andreae, M. O., Artaxo, P., and Maenhaut, W.: Formation of secondary
772 organic aerosols through photooxidation of isoprene, Science, 303(5661), 1173–1176,
773 2004.
774 Claeys, M., Szmigielski, R., Kourtchev, I., van der Veken, P., Vermeylen, R., Maenhaut, W.,
775 Jaoui, M., Kleindienst, T. E., Lewandowski, M., Offenberg, J., and Edney, E. O.:
776 Hydroxydicarboxylic acids: Markers for secondary organic aerosol from the
777 photooxidation of α-pinene, Environ. Sci. Technol., 41(5), 1628–1634, 2007.
778 Conte, L., Szopa, S., Aumont, O., Gros, V., and Bopp, L.: Sources and sinks of isoprene in
779 the global open ocean: Simulated patterns and emissions to the atmosphere, J. Geophys.
780 Res. Ocean., 9, e2019JC015946, https://doi.org/10.1029/2019JC015946, 2020.
781 Deguillaume, L., Leriche, M., Amato, P., Ariya, P. A., Delort, A.-M., Pöschl, U.,
782 Chaumerliac, N., Bauer, H., Flossmann, A. I., and Morris, C. E.: Microbiology and
783 atmospheric processes: chemical interactions of primary biological aerosols,
784 Biogeosciences, 5, 1073–1084, 2008.
785 Ding, X., Wang, X. M., Gao, B., Fu, X. X., He, Q. F., Zhao, X. Y., Yu, J. Z., and Zheng, M.:
786 Tracer-based estimation of secondary organic carbon in the Pearl River Delta, south
787 China, J. Geophys. Res. Atmos., 117, D05313, https://doi.org/10.1029/2011JD016596,
788 2012.
789 Ding, X., He, Q. F., Shen, R. Q., Yu, Q. Q., and Wang, X. M.: Spatial distributions of
790 secondary organic aerosols from isoprene, monoterpenes, β-caryophyllene, and aromatics
791 over China during summer, J. Geophys. Res., 119, 11877-11891,
792 https://doi.org/10.1002/2014JD021748, 2014.
793 Engling, G., Carrico, C. M., Kreldenweis, S. M., Collett, J. L., Day, D. E., Malm, W. C.,
794 Lincoln, E., Hao, W. M., Iinuma, Y., and Herrmann, H.: Determination of levoglucosan

in biomass combustion aerosol by high-performance anion-exchange chromatography with pulsed amperometric detection, Atmos. Environ., 40, S299–S311, 2006.

Engling, G., Lee, J. J., Tsai, Y. W., Lung, S. C. C., Chou, C. C. K., and Chan, C. Y.: Size-resolved anhydrosugar composition in smoke aerosol from controlled field burning of rice straw, Aerosol Sci. Technol., 43(7), 662–672, https://doi.org/10.1080/02786820902825113, 2009.

Fabbri, D., Marynowski, L., Fabianska, M. J., Zaton, M., and Simoneit, B. R. T.: Levoglucosan and other cellulose markers in pyrolysates of miocene lignites: Geochemical and environmental implications, Environ. Sci. Technol., 42(8), 2957–2963, https://doi.org/10.1021/Es7021472, 2008.

Fine, P. M., Cass, G. R., and Simoneit, B. R. T.: Chemical characterization of fine particle emissions from fireplace combustion of woods grown in the northeastern United States, Environ. Sci. Technol., 35(13), 2665–2675, 2001.

Fine, P. M., Cass, G. R., and Simoneit, B. R. T.: Chemical characterization of fine particle emissions from the fireplace combustion of wood types grown in the Midwestern and Western United States, Environ. Eng. Sci., 21(3), 387–409, 2004.

Fraser, M. P. and Lakshmanan, K.: Using levoglucosan as a molecular marker for the long-range transport of biomass combustion aerosols, Environ. Sci. Technol., 34(21), 4560–4564, https://doi.org/10.1021/es991229l, 2000.

Fu, P., Kawamura, K., Kanaya, Y., and Wang, Z.: Contributions of biogenic volatile organic compounds to the formation of secondary organic aerosols over Mt. Tai, Central East China, Atmos. Environ., 44, 4817-4826, https://doi.org/10.1016/j.atmosenv.2010.08.040, 2010a.

Fu, P., Kawamura, K., Kobayashi, M., and Simoneit, B. R. T.: Seasonal variations of sugars in atmospheric particulate matter from Gosan, Jeju Island: Significant contributions of airborne pollen and Asian dust in spring, Atmos. Environ., 55, 234–239, https://doi.org/10.1016/j.atmosenv.2012.02.061, 2012a.

Fu, P. Q., Kawamura, K., Okuzawa, K., Aggarwal, S. G., Wang, G., Kanaya, Y., and Wang, Z.: Organic molecular compositions and temporal variations of summertime mountain aerosols over Mt. Tai, North China Plain, J. Geophys. Res. Atmos., 113, D1910, https://doi.org/10.1029/2008JD009900, 2008.

Fu, P. Q., Kawamura, K., and Barrie, L. A.: Photochemical and other sources of organic compounds in the Canadian high Arctic aerosol pollution during winter-spring, Environ. Sci. Technol., 43(2), 286–292, 2009a.

Fu, P. Q., Kawamura, K., Chen, J., and Barrie, L. A.: Isoprene, monoterpene, and sesquiterpene oxidation products in the high Arctic aerosols during late winter to early summer, Environ. Sci. Technol., 43(11), 4022–4028, 2009b.

Fu, P. Q., Kawamura, K., Pavuluri, C. M., Swaminathan, T., and Chen, J.: Molecular characterization of urban organic aerosol in tropical India: contributions of primary emissions and secondary photooxidation, Atmos. Chem. Phys., 10(6), 2663–2689, 2010b.

Fu, P. Q., Kawamura, K., and Miura, K.: Molecular characterization of marine organic aerosols collected during a round-the-world cruise, J. Geophys. Res., 116, D13302, https://doi.org/10.1029/2011jd015604, 2011.

838 Fu, P. Q., Kawamura, K., Chen, J., Li, J., Sun, Y. L., Liu, Y., Tachibana, E., Aggarwal, S. G.,
839 Okuzawa, K., Tanimoto, H., Kanaya, Y., and Wang, Z. F.: Diurnal variations of organic
840 molecular tracers and stable carbon isotopic composition in atmospheric aerosols over
841 Mt. Tai in the North China Plain: an influence of biomass burning, Atmos. Chem. Phys.,
842 12(18), 8359–8375, https://doi.org/10.5194/Acp-12-8359-2012, 2012b.
843 Gómez-González, Y., Wang, W., Vermeylen, R., Chi, X., Neirynck, J., Janssens, I. A.,
844 Maenhaut, W., and Claeys, M.: Chemical characterisation of atmospheric aerosols during
845 a 2007 summer field campaign at Brasschaat, Belgium: Sources and source processes of
846 biogenic secondary organic aerosol, Atmos. Chem. Phys., 12, 125-138,
847 https://doi.org/10.5194/acp-12-125-2012, 2012.
848 Graham, B., Guyon, P., Taylor, P. E., Artaxo, P., Maenhaut, W., Glovsky, M. M., Flagan, R.
849 C., and Andreae, M. O.: Organic compounds present in the natural Amazonian aerosol:
850 Characterization by gas chromatography-mass spectrometry, J. Geophys. Res. Atmos.,
851 108, D24, 4766, https://doi.org/10.1029/2003JD003990, 2003.
852 Griffin, R. J., Cocker, D. R., Seinfeld, J. H., and Dabdub, D.: Estimate of global atmospheric
853 organic aerosol from oxidation of biogenic hydrocarbons, Geophys. Res. Lett., 26, 2721–
854 2724, 1999.
855 Guenther, A., Hewitt, C. N., Erickson, D., Fall, R., Geron, C., Graedel, T., Harley, P.,
856 Klinger, L., Lerdau, M., McKay, W. A., Pierce, T., Scholes, B. R. S., Tallamraju, R.,
857 Taylor, J., and Zimmerman, P.: A global model of natural volatile organic compound
858 emissions, J. Geophys. Res., 100(D5), 8873–8892, 1995.
859 Guenther, A., Karl, T., Harley, P., Wiedinmyer, C., Palmer, P. I., and Geron, C.: Estimates of
860 global terrestrial isoprene emissions using MEGAN (Model of Emissions of Gases and
861 Aerosols from Nature), Atmos. Chem. Phys., 6, 3181–3210, 2006.
862 Haque, M. M., Kawamura, K., Deshmukh, D. K., Fang, C., Song, W., Mengying, B., and
863 Zhang, Y. L.: Characterization of organic aerosols from a Chinese megacity during
864 winter: Predominance of fossil fuel combustion, Atmos. Chem. Phys., 19, 5147-5164,
865 https://doi.org/10.5194/acp-19-5147-2019, 2019.
866 Heald, C. L., and Spracklen, D. V.: Atmospheric budget of primary biological aerosol
867 particles from fungal spores, Geophys. Res. Lett., 36, L09806,
868 https://doi.org/10.1029/2009GL037493, 2009.
869 Heald, C. L., Henze, D. K., Horowitz, L. W., Feddema, J., Lamarque, J. F., Guenther, A.,
870 Hess, P. G., Vitt, F., Seinfeld, J. H., Goldstein, A. H., and Fung, I.: Predicted change in
871 global secondary organic aerosol concentrations in response to future climate, emissions,
872 and land use change, J. Geophys. Res., 113(D5), https://doi.org/10.1029/2007jd009092,
873 2008.
874 Hennigan, C. J., Sullivan, A. P., Collett, J. L., and Robinson, A. L.: Levoglucosan stability in
875 biomass burning particles exposed to hydroxyl radicals, Geophys. Res. Lett., 37,
876 https://doi.org/10.1029/2010GL043088, 2010.
877 Hu, Q. H., Xie, Z. Q., Wang, X. M., Kang, H., He, Q. F., and Zhang, P.: Secondary organic
878 aerosols over oceans via oxidation of isoprene and monoterpenes from Arctic to
879 Antarctic, Sci. Rep., 3, 3119, https://doi.org/10.1038/srep02280, 2013.
880 Huebert, B. J., Bates, T., Russell, P. B., Shi, G. Y., Kim, Y. J., Kawamura, K., Carmichael,
881 G., and Nakajima, T.: An overview of ACE-Asia: Strategies for quantifying the

882 relationships between Asian aerosols and their climatic impacts, J. Geophys. Res. Atmos.,
883 108(D23), 8633, https://doi.org/10.1029/2003JD003550, 2003.
884 Jia, Y. L. and Fraser, M.: Characterization of saccharides in size-fractionated ambient
885 particulate matter and aerosol sources: The contribution of primary biological aerosol
886 particles (PBAPs) and soil to ambient particulate matter, Environ. Sci. Technol., 45(3),
887 930–936, https://doi.org/10.1021/es103104e, 2011.
888 Kanakidou, M., Seinfeld, J. H., Pandis, S. N., Barnes, I., Dentener, F. J., Facchini, M. C., Van
889 Dingenen, R., Ervens, B., Nenes, A., Nielsen, C. J., Swietlicki, E., Putaud, J. P.,
890 Balkanski, Y., Fuzzi, S., Horth, J., Moortgat, G. K., Winterhalter, R., Myhre, C. E. L.,
891 Tsigaridis, K., Vignati, E., Stephanou, E. G., and Wilson, J.: Organic aerosol and global
892 climate modelling: a review, Atmos. Chem. Phys., 5, 1053–1123, 2005.
893 Kang, M., Ren, L., Ren, H., Zhao, Y., Kawamura, K., Zhang, H., Wei, L., Sun, Y., Wang, Z.,
894 and Fu, P.: Primary biogenic and anthropogenic sources of organic aerosols in Beijing,
895 China: Insights from saccharides and n-alkanes, Environ. Pollut., 243, 1579-1587,
896 https://doi.org/10.1016/j.envpol.2018.09.118, 2018a.
897 Kang, M., Fu, P., Kawamura, K., Yang, F., Zhang, H., Zang, Z., Ren, H., Ren, L., Zhao, Y.,
898 Sun, Y., and Wang, Z.: Characterization of biogenic primary and secondary organic
899 aerosols in the marine atmosphere over the East China Sea, Atmos. Chem. Phys., 19,
900 13947-13967, https://doi.org/10.5194/acp-18-13947-2018, 2018b.
901 Kawamura, K., Kobayashi, M., Tsubonuma, N., Mochida, M., Watanabe, T., and Lee, M.:
902 Organic and inorganic compositions of marine aerosols from East Asia: Seasonal
903 variations of water-soluble dicarboxylic acids, major ions, total carbon and nitrogen, and
904 stable C and N isotopic composition, in geochemical investigations in earth and space
905 science: A Tribute to Isaac R. Kaplan, edited by R. J. Hill, J. Leventhal, Z. Aizenshtat, M.
906 J. Baedecker, G. Claypool, R. Eganhouse, M. Goldhaber, and K. Peters, pp. 243–265, The
907 Geochemical Society, 2004.
908 Kessler, S. H., Smith, J. D., Che, D. L., Worsnop, D. R., Wilson, K. R., and Kroll, J. H.:
909 Chemical sinks of organic aerosol: Kinetics and products of the heterogeneous oxidation
910 of erythritol and levoglucosan, Environ. Sci. Technol., 44(18), 7005–7010,
911 https://doi.org/10.1021/Es101465m, 2010.
912 Kourtchev, I., Hellebust, S., Bell, J. M., O'Connor, I. P., Healy, R. M., Allanic, A., Healy, D.,
913 Wenger, J. C., and Sodeau, J. R.: The use of polar organic compounds to estimate the
914 contribution of domestic solid fuel combustion and biogenic sources to ambient levels of
915 organic carbon and $PM_{2.5}$ in Cork Harbour, Ireland, Sci. Total Environ., 11, 2143-2155,
916 https://doi.org/10.1016/j.scitotenv.2011.02.027, 2011.
917 Kroll, J. H., Ng, N. L., Murphy, S. M., Flagan, R. C., and Seinfeld, J. H.: Secondary organic
918 aerosol formation from isoprene photooxidation under high-NOx conditions, Geophys.
919 Res. Lett., 32(18), L18808, https://doi.org/10.1029/2005gl023637, 2005.
920 Kroll, J. H., Ng, N. L., Murphy, S. M., Flagan, R. C., and Seinfeld, J. H.: Secondary organic
921 aerosol formation from isoprene photooxidation, Environ. Sci. Technol., 40, 1869–1877,
922 2006.
923 Kundu, S., Kawamura, K., and Lee, M.: Seasonal variations of diacids, ketoacids, and α-
924 dicarbonyls in aerosols at Gosan, Jeju Island, South Korea: Implications for sources,

925 formation, and degradation during long-range transport, J. Geophys. Res., 115, D19307,
926 https://doi.org/10.1029/2010jd013973, 2010.
927 Lewis, D. H. and Smith, D. C.: Sugar alcohols (polyols) in fungi and green plants: 1.
928 Distributions, physiology and metabolism, New Phytol., 66, 143–184, 1967.
929 Liu, J., Chu, B., Chen, T., Liu, C., Wang, L., Bao, X., and He, H.: Secondary organic aerosol
930 formation from ambient air at an urban site in Beijing: Effects of OH exposure and
931 precursor concentrations, Environ. Sci. Technol., 52, 6834-6841,
932 https://doi.org/10.1021/acs.est.7b05701, 2018.
933 Medeiros, P. M. and Simoneit, B. R. T.: Analysis of sugars in environmental samples by gas
934 chromatography-mass spectrometry, J. Chromatogr. A, 1141(2), 271–278,
935 https://doi.org/10.1016/j.chroma.2006.12.017, 2007.
936 Medeiros, P. M., Conte, M. H., Weber, J. C., and Simoneit, B. R. T.: Sugars as source
937 indicators of biogenic organic carbon in aerosols collected above the Howland
938 Experimental Forest, Maine, Atmos. Environ., 40(9), 1694–1705, 2006.
939 Mohn, J., Szidat, S., Fellner, J., Rechberger, H., Quartier, R., Buchmann, B., and
940 Emmenegger, L.: Determination of biogenic and fossil CO_2 emitted by waste incineration
941 based on $^{14}CO_2$ and mass balances, Bioresour. Technol., 99, 6471-6479,
942 https://doi.org/10.1016/j.biortech.2007.11.042, 2008.
943 Müller, L., Reinnig, M. C., Naumann, K. H., Saathoff, H., Mentel, T. F., Donahue, N. M.,
944 and Hoffmann, T.: Formation of 3-methyl-1,2,3-butanetricarboxylic acid via gas phase
945 oxidation of pinonic acid - A mass spectrometric study of SOA aging, Atmos. Chem.
946 Phys., 12, 1483-1496, https://doi.org/10.5194/acp-12-1483-2012, 2012.
947 Nakajima, T., Yoon, S. C., Ramanathan, V., Shi, G. Y., Takemura, T., Higurashi, A.,
948 Takamura, T., Aoki, K., Sohn, B. J., Kim, S. W., Tsuruta, H., Sugimoto, N., Shimizu, A.,
949 Tanimoto, H., Sawa, Y., Lin, N. H., Lee, C. T., Goto, D., and Schutgens, N.: Overview of
950 the atmospheric brown cloud east Asian regional experiment 2005 and a study of the
951 aerosol direct radiative forcing in east Asia, J. Geophys. Res. Atmos., 112, D24S91,
952 https://doi.org/10.1029/2007JD009009, 2007.
953 Ng, N. L., Kwan, A. J., Surratt, J. D., Chan, A. W. H., Chhabra, P. S., Sorooshian, A., Pye, H.
954 O. T., Crounse, J. D., Wennberg, P. O., Flagan, R. C., and Seinfeld, J. H.: Secondary
955 organic aerosol (SOA) formation from reaction of isoprene with nitrate radicals (NO_3),
956 Atmos. Chem. Phys., 8(14), 4117–4140, 2008.
957 Offenberg, J., Lewis, C., Lewandowski, M., Jaoui, M., Kleindienst, T. E., and Edney, E. O.:
958 Contributions of toluene and α-pinene to SOA formed in an irradiated toluene/r-
959 pinene/NOx/air mixture: Comparison of results using ^{14}C content and SOA organic tracer
960 methods, Environ. Sci. Tec., 41, 3972–3976, 2007.
961 Pashynska, V., Vermeylen, R., Vas, G., Maenhaut, W., and Claeys, M.: Development of a gas
962 chromatographic/ion trap mass spectrometric method for the determination of
963 levoglucosan and saccharidic compounds in atmospheric aerosols. Application to urban
964 aerosols, J. Mass Spectrom., 37(12), 1249–1257, 2002.
965 Pio, C., Legrand, M., Alves, C. A., Oliveira, T., Afonso, J., Caseiro, A., Puxbaum, H.,
966 Sánchez-Ochoa, A., and Gelencsér, A.: Chemical composition of atmospheric aerosols
967 during the 2003 summer intense forest fire period, Atmos. Environ., 42, 7530–7543,
968 2008.

969 Ramanathan, V., Li, F., Ramana, M. V., Praveen, P. S., Kim, D., Corrigan, C. E., Nguyen, H.,
970 Stone, E. A., Schauer, J. J., Carmichael, G. R., Adhikary, B., and Yoon, S. C.:
971 Atmospheric brown clouds: Hemispherical and regional variations in long-range
972 transport, absorption, and radiative forcing, J. Geophys. Res. Atmos., 112, D22S21,
973 https://doi.org/10.1029/2006JD008124, 2007.
974 Robinson, A. L., Donahue, N. M., Shrivastava, M. K., Weitkamp, E. A., Sage, A. M.,
975 Grieshop, A. P., Lane, T. E., Pierce, J. R., and Pandis, S. N.: Rethinking organic aerosols:
976 Semivolatile emissions and photochemical aging, Science, 315, 1259–1262, 2007.
977 Salazar, G., Zhang, Y. L., Agrios, K., and Szidat, S.: Development of a method for fast and
978 automatic radiocarbon measurement of aerosol samples by online coupling of an
979 elemental analyzer with a MICADAS AMS, Nucl. Instruments Methods Phys. Res. Sect.
980 B Beam Interact. with Mater. Atoms, 361, 163-167,
981 https://doi.org/10.1016/j.nimb.2015.03.051, 2015.
982 Schmidl, C., Marr, I. L., Caseiro, A., Kotianova, P., Berner, A., Bauer, H., Kasper-Giebl, A.,
983 and Puxbaum, H.: Chemical characterisation of fine particle emissions from wood stove
984 combustion of common woods growing in mid-European Alpine regions, Atmos.
985 Environ., 42, 126–141, 2008a.
986 Schmidl, C., Bauer, H., Dattler, A., Hitzenberger, R., Weissenboeck, G., Marr, I. L., and
987 Puxbaum, H.: Chemical characterisation of particle emissions from burning leaves,
988 Atmos. Environ., 42(40), 9070–9079, https://doi.org/10.1016/J.Atmosenv.2008.09.010,
989 2008b.
990 Shaw, S. L., Gantt, B., and Meskhidze, N.: Production and emissions of marine isoprene and
991 monoterpenes: A Review, Adv. Meteorol., 2010, 408696,
992 https://doi.org/10.1155/2010/408696, 2010.
993 Simoneit, B. R. T.: Biomass burning-a review of organic tracers for smoke from incomplete
994 combustion, Appl. Geochem., 17, 129–162, 2002.
995 Simoneit, B. R. T., Elias, V. O., Kobayashi, M., Kawamura, K., Rushdi, A. I., Medeiros, P.
996 M., Rogge, W. F., and Didyk, B. M.: Sugars-dominant water-soluble organic compounds
997 in soils and characterization as tracers in atmospheric particulate matter, Environ. Sci.
998 Technol., 38(22), 5939–5949, 2004a.
999 Simoneit, B. R. T., Kobayashi, M., Mochida, M., Kawamura, K., Lee, M., Lim, H-J., Turpin,
1000 B. J., and Komazaki, Y.: Composition and major sources of organic compounds of
1001 aerosol particulate matter sampled during the ACE-Asia campaign, J. Geophys. Res.,
1002 109(D19), D19S10, https://doi.org/10.1029/2004jd004598, 2004b.
1003 Simoneit, B. R. T., Schauer, J. J., Nolte, C. G., Oros, D. R., Elias, V. O., Fraser, M. P.,
1004 Rogge, W. F., and Cass, G. R.: Levoglucosan, a tracer for cellulose in biomass burning
1005 and atmospheric particles, Atmos. Environ., 33(2), 173–182,
1006 https://doi.org/10.1016/S1352-2310(98)00145-9, 1999.
1007 Singh, N., Mhawish, A., Deboudt, K., Singh, R. S., and Banerjee, T.: Organic aerosols over
1008 Indo-Gangetic Plain: Sources, distributions and climatic implications, Atmos. Environ.,
1009 157, 59-74, https://doi.org/10.1016/j.atmosenv.2017.03.008, 2017.
1010 Stein, A. F., Draxler, R. R., Rolph, G. D., Stunder, B. J. B., Cohen, M. D., and Ngan, F.:
1011 Noaa's hysplit atmospheric transport and dispersion modeling system, Bull. Am.
1012 Meteorol. Soc., 96, 2059-2077, https://doi.org/10.1175/BAMS-D-14-00110.1, 2015.

1013 Stuiver, M. and Polach, H. A.: Discussion: Reporting of ^{14}C data, Radiocarbon, 19(3),
1014 355−363, 1997.
1015 Sullivan, A. P., Holden, A. S., Patterson, L. A., McMeeking, G. R., Kreidenweis, S. M.,
1016 Malm, W. C., Hao, W. M., Wold, C. E., and Collett, Jr., J. L.: A method for smoke
1017 marker measurements and its potential application for determining the contribution of
1018 biomass burning from wildfires and prescribed fires to ambient $PM_{2.5}$ organic carbon, J.
1019 Geophys. Res., 113, D22302, https://doi.org/10.1029/2008JD010216, 2008.
1020 Surratt, J. D., Murphy, S. M., Kroll, J. H., Ng, N. L., Hildebrandt, L., Sorooshian, A.,
1021 Szmigielski, R., Vermeylen, R., Maenhaut, W., Claeys, M., Flagan, R. C., and Seinfeld, J.
1022 H.: Chemical composition of secondary organic aerosol formed from the photooxidation
1023 of isoprene, J. Phys. Chem. A, 110(31), 9665–9690, 2006.
1024 Surratt, J. D., Chan, A. W. H., Eddingsaas, N. C., Chan, M. N., Loza, C. L., Kwan, A. J.,
1025 Hersey, S. P., Flagan, R. C., Wennberg, P. O., and Seinfeld, J. H.: Reactive intermediates
1026 revealed in secondary organic aerosol formation from isoprene, Proc. Natl. Acad. Sci.
1027 USA, 107(15), 6640–6645, 2010.
1028 Szidat, S., Jenk, T. M., Synal, H. A., Kalberer, M., Wacker, L., Hajdas, I., Kasper-Giebl, A.,
1029 and Baltensperger, U.: Contributions of fossil fuel, biomass-burning, and biogenic
1030 emissions to carbonaceous aerosols in Zurich as traced by ^{14}C, J. Geophys. Res. Atmos.,
1031 111, D07206, https://doi.org/10.1029/2005JD006590, 2006.
1032 Szmigielski, R., Surratt, J. D., Gómez-González, G., Van der Veken, P., Kourtchev, I.,
1033 Vermeylen, R., Blockhuys, F., Jaoui, M., Kleindienst, T. E., Lewandowski, M.,
1034 Offenberg, J. H., Edney, E. O., Seinfeld, J. H., Maenhaut, W., and Claeys, M.: 3-Methyl-
1035 1,2,3-butanetricarboxylic acid: An atmospheric tracer for terpene secondary organic
1036 aerosol, Geophys. Res. Lett., 34, L24811, https://doi.org/10.1029/2007GL031338, 2007.
1037 Theodosi, C., Panagiotopoulos, C., Nouara, A., Zarmpas, P., Nicolaou, P., Violaki, K.,
1038 Kanakidou, M., Sempéré, R., and Mihalopoulos, N.: Sugars in atmospheric aerosols over
1039 the Eastern Mediterranean, Prog. Oceanogr., 163, Special Issue: SI, 70-81,
1040 https://doi.org/10.1016/j.pocean.2017.09.001, 2018.
1041 Tyagi, P., Kawamura, K., Kariya, T., Bikkina, S., Fu, P., and Lee, M.: Tracing atmospheric
1042 transport of soil microorganisms and higher plant waxes in the East Asian outflow to the
1043 North Pacific Rim by using hydroxy fatty acids: Year-round observations at Gosan, Jeju
1044 Island, J. Geophys. Res., 122, 4112-4131, https://doi.org/10.1002/2016JD025496, 2017.
1045 Verma, S. K., Kawamura, K., Chen, J., Fu, P., and Zhu, C.: Thirteen years of observations on
1046 biomass burning organic tracers over Chichijima Island in the western North Pacific: An
1047 outflow region of Asian aerosols, J. Geophys. Res., 120, 4155-4168,
1048 https://doi.org/10.1002/2014JD022224, 2015.
1049 Verma, S. K., Kawamura, K., Chen, J., and Fu, P.: Thirteen years of observations on primary
1050 sugars and sugar alcohols over remote Chichijima Island in the western North Pacific,
1051 Atmos. Chem. Phys., 18, 81-101, https://doi.org/10.5194/acp-18-81-2018, 2018.
1052 Wang, G. and Kawamura, K.: Molecular characteristics of urban organic aerosols from
1053 Nanjing: A case study of a mega-city in China, Environ. Sci. Technol., 39(19), 7430–
1054 7438, 2005.

Wang, G. H., Kawamura, K., and Lee, M.: Comparison of organic compositions in dust storm and normal aerosol samples collected at Gosan, Jeju Island, during spring 2005, Atmos. Environ., 43(2), 219–227, https://doi.org/10.1016/J.Atmosenv.2008.09.046, 2009a.

Wang, G. H., Li, J. J., Cheng, C. L., Zhou, B. H., Xie, M. J., Hu, S. Y., Meng, J. J., Sun, T., Ren, Y. Q., Cao, J. J., Liu, S. X., Zhang, T., and Zhao, Z. Z.: Observation of atmospheric aerosols at Mt. Hua and Mt. Tai in central and east China during spring 2009-Part 2: Impact of dust storm on organic aerosol composition and size distribution, Atmos. Chem. Phys., 12(9), 4065–4080, 2012.

Wang, W., Kourtchev, I., Graham, B., Cafmeyer, J., Maenhaut, W., and Claeys, M.: Characterization of oxygenated derivatives of isoprene related to 2-methyltetrols in Amazonian aerosols using trimethylsilylation and gas chromatography/ion trap mass spectrometry, Rapid Commun. Mass Spectrom., 19, 1343–1351, 2005.

Wang, Y. Q., Zhang, X. Y., and Draxler, R. R.: TrajStat: GIS-based software that uses various trajectory statistical analysis methods to identify potential sources from long-term air pollution measurement data, Environ. Model. Softw., 24, 938-939, https://doi.org/10.1016/j.envsoft.2009.01.004, 2009b.

Wu, J., Kong, S., Zeng, X., Cheng, Y., Yan, Q., Zheng, H., Yan, Y., Zheng, S., Liu, D., Zhang, X., Fu, P., Wang, S., and Qi, S.: First high-resolution emission inventory of levoglucosan for biomass burning and non-biomass burning sources in China, Environ. Sci. Technol., 55, 3, 1497–1507, 2021.

Yan, C., Zheng, M., Sullivan, A. P., Shen, G., Chen, Y., Wang, S., Zhao, B., Cai, S., Desyaterik, Y., Li, X., Zhou, T., Gustafsson, Ö., and Collett, J. L.: Residential coal combustion as a source of levoglucosan in China, Environ. Sci. Technol., 52, 3, 1665–1674, https://doi.org/10.1021/acs.est.7b05858, 2018.

Yttri, K. E., Dye, C., and Kiss, G.: Ambient aerosol concentrations of sugars and sugar-alcohols at four different sites in Norway, Atmos. Chem. Phys., 7, 4267–4279, 2007.

Zangrando, R., Barbaro, E., Kirchgeorg, T., Vecchiato, M., Scalabrin, E., Radaelli, M., Đorđević, D., Barbante, C., and Gambaro, A.: Five primary sources of organic aerosols in the urban atmosphere of Belgrade (Serbia), Sci. Total Environ., 571, 1441-1453, https://doi.org/10.1016/j.scitotenv.2016.06.188, 2016.

Zhang, Y. L., Perron, N., Ciobanu, V. G., Zotter, P., Minguillón, M. C., Wacker, L., Prévôt, A. S. H., Baltensperger, U., and Szidat, S.: On the isolation of OC and EC and the optimal strategy of radiocarbon-based source apportionment of carbonaceous aerosols, Atmos. Chem. Phys., 12, 10841-10856, https://doi.org/10.5194/acp-12-10841-2012, 2012.

Zhang, Y. L., Huang, R. J., El Haddad, I., Ho, K. F., Cao, J. J., Han, Y., Zotter, P., Bozzetti, C., Daellenbach, K. R., Canonaco, F., Slowik, J. G., Salazar, G., Schwikowski, M., Schnelle-Kreis, J., Abbaszade, G., Zimmermann, R., Baltensperger, U., Prévôt, A. S. H., and Szidat, S.: Fossil vs. non-fossil sources of fine carbonaceous aerosols in four Chinese cities during the extreme winter haze episode of 2013, Atmos. Chem. Phys., 15(3), 1299-1312, https://doi.org/10.5194/acp-15-1299-2015, 2015.

Zhang, Y. L., Kawamura, K., Agrios, K., Lee, M., Salazar, G., and Szidat, S.: Fossil and nonfossil sources of organic and elemental carbon aerosols in the outflow from Northeast China, Environ. Sci. Technol., 50, 6284-6292, https://doi.org/10.1021/acs.est.6b00351, 2016.

Zhu, C., Kawamura, K., and Kunwar, B.: Effect of biomass burning over the western North Pacific Rim: wintertime maxima of anhydrosugars in ambient aerosols from Okinawa., Atmos. Chem. Phys., 15, 1959–1973, https://doi.org/10.5194/acp-15-1959-2015, 2015a.

Zhu, C., Kawamura, K., and Kunwar, B.: Organic tracers of primary biological aerosol particles at subtropical Okinawa island in the western North pacific rim, J. Geophys. Res., 120, 5504-5523, https://doi.org/10.1002/2015JD023611, 2015b.

1126 **Table 1.** Concentrations of identified sugar compounds and BSOA tracers (ng m^{-3}) in the atmospheric
1127 aerosol samples from Gosan.

Species	Annual	Summer	Fall	Winter	Spring
	Avg.[a] ± S.D.[b] Min.[c], Max.[d]	Avg. ± S.D. Min., Max.	Avg. ± S.D. Min., Max.	Avg. ± S.D. Min., Max.	Avg. ± S.D. Min., Max.
Anhydrosugars					
Levoglucosan (Lev)	17.6 ± 16.8 0.60, 45.9	2.92 ± 3.89 0.60, 9.81	21.7 ± 19.0 2.30, 43.9	39.2 ± 6.60 32.0, 45.9	12.7 ± 11.6 1.45, 33.4
Mannosan (Man)	1.57 ± 1.82 0.05, 6.74	0.18 ± 0.24 0.05, 0.61	1.69 ± 1.49 0.13, 3.66	3.63 ± 2.28 1.47, 6.74	1.31 ± 1.57 0.08, 4.08
Galactosan (Gal)	2.28 ± 2.10 0.14, 6.78	0.64 ± 0.68 0.14, 1.82	2.45 ± 2.13 0.35, 4.92	5.21 ± 1.64 3.40, 6.78	1.65 ± 1.26 0.50, 3.88
Primary Sugars					
Glucose	18.8 ± 27.1 2.45, 122	13.4 ± 18.2 2.45, 45.6	16.5 ± 15.7 2.68, 33.6	4.74 ± 3.14 2.88, 9.44	32.4 ± 41.1 4.87, 122
Fructose	10.3 ± 15.9 0.97, 74.0	4.90 ± 5.15 0.97, 13.7	7.48 ± 6.99 1.71, 16.2	3.82 ± 4.45 1.56, 10.5	19.8 ± 25.0 2.69, 74.0
Sucrose	16.1 ± 32.2 0.26, 140	1.46 ± 1.05 0.68, 3.28	9.74 ± 12.1 0.76, 27.2	8.87 ± 16.3 0.42, 33.3	35.1 ± 50.5 0.26, 140
Trehalose	2.42 ± 1.97 0.65, 7.03	2.72 ± 2.53 0.97, 6.98	3.71 ± 2.29 1.18, 7.03	1.21 ± 0.42 0.72, 1.63	1.98 ± 1.55 0.65, 5.33
Xylose	0.81 ± 0.65 0.04, 2.03	0.23 ± 0.23 0.04, 0.63	0.86 ± 0.68 0.14, 1.70	1.59 ± 0.37 1.21, 2.03	0.74 ± 0.55 0.16, 1.68
Sugar alcohols					
Arabitol	3.96 ± 4.24 0.47, 18.7	5.64 ± 7.46 1.20, 18.7	5.27 ± 3.51 2.27, 10.9	1.06 ± 0.60 0.47, 1.91	3.47 ± 2.19 1.18, 6.30
Mannitol	4.61 ± 5.54 0.25, 22.0	7.39 ± 8.65 1.71, 22.0	6.64 ± 6.03 1.69, 16.7	0.99 ± 0.45 0.55, 1.60	3.24 ± 2.67 0.25, 7.03
Erythritol	0.62 ± 0.43 0.12, 1.52	0.92 ± 0.53 0.42, 1.52	0.93 ± 0.33 0.55, 1.27	0.42 ± 0.27 0.16, 0.80	0.30 ± 0.12 0.12, 0.48
Inositol	0.34 ± 0.39 0.04, 1.53	0.29 ± 0.41 0.08, 1.03	0.56 ± 0.60 0.10, 1.53	0.13 ± 0.07 0.08, 0.23	0.35 ± 0.28 0.04, 0.73
Isoprene SOA tracers					
2-MGA	0.99 ± 0.70 0.17, 2.79	1.61 ± 1.17 0.17, 2.79	0.95 ± 0.43 0.51, 1.61	0.67 ± 0.14 0.49, 0.81	0.76 ± 0.35 0.20, 1.32
Σ2-MLTs	1.04 ± 1.40 0.05, 5.81	2.48 ± 1.98 0.51, 5.81	1.34 ± 1.16 0.33, 2.74	0.20 ± 0.05 0.15, 0.26	0.29 ± 0.25 0.05, 0.82
ΣC5-alkene triols	0.20 ± 0.25 0.02, 1.17	0.46 ± 0.44 0.02, 1.17	0.13 ± 0.05 0.05, 0.18	0.09 ± 0.03 0.05, 0.13	0.14 ± 0.11 0.02, 0.30
Monoterpene SOA tracers					
cis-pinonic acid	0.15 ± 0.14 0.02, 0.52	0.12 ± 0.13 0.03, 0.36	0.08 ± 0.06 0.02, 0.16	0.07 ± 0.03 0.02, 0.10	0.26 ± 0.17 0.08, 0.52
pinic acid	1.67 ± 1.01 0.72, 4.81	2.40 ± 1.67 0.99, 4.81	1.53 ± 0.57 0.75, 2.11	1.07 ± 0.25 0.84, 1.42	1.61 ± 0.78 0.72, 2.94
3-HGA	2.30 ± 2.38 0.19, 10.6	3.46 ± 4.39 0.19, 10.6	1.52 ± 0.77 0.76, 2.79	1.40 ± 0.39 0.94, 1.88	2.54 ± 1.83 0.38, 4.57
MBTCA	5.11 ± 4.54 0.29, 19.6	8.44 ± 6.88 3.00, 19.6	6.24 ± 3.64 1.17, 9.49	1.90 ± 0.85 0.97, 2.83	3.77 ± 2.96 0.29, 8.08

[a]Average, [b]Standard deviation, [c]Minimum, [d]Maximum. 2-MGA: 2-methylglyceric acid, 2-MLTs: 2-methyltetrols, 3-HGA: 3-hydroxyglutaric acid, MBTCA: 3-methyl-1,2,3-butanetricarboxylic acid.

1128

1129 **Table 2.** Statistical summary of diagnostic ratios and carbonaceous components contribution in Gosan
1130 aerosols.
1131

Species	Annual	Summer	Fall	Winter	Spring
	Avg.[a] ± S.D.[b] Min.[c], Max.[d]	Avg. ± S.D. Min., Max.	Avg. ± S.D. Min., Max.	Avg. ± S.D. Min., Max.	Avg. ± S.D. Min., Max.
Diagnostic ratios					
Lev/Man	15.1 ± 6.76 6.81, 31.3	17.1 ± 8.21 8.58, 28.4	13.7 ± 2.51 11.1, 17.3	13.5 ± 6.24 6.81, 21.7	15.4 ± 8.76 6.98, 31.3
Man/Gal	0.55 ± 0.32 0.10, 1.07	0.28 ± 0.13 0.10, 0.42	0.64 ± 0.20 0.37, 0.90	0.66 ± 0.27 0.43, 1.05	0.61 ± 0.43 0.16, 1.07
Lev/(Man + Gal)	4.27 ± 1.23 2.18, 6.56	3.12 ± 0.78 2.18, 4.03	5.08 ± 0.32 4.71, 5.51	4.85 ± 1.35 3.49, 6.56	4.17 ± 1.33 2.50, 6.45
Lev/$K^+ \times 10^{-2}$	5.73 ± 5.65 0.65, 23.2	1.00 ± 0.52 0.65, 1.91	3.94 ± 2.51 1.26, 6.30	12.3 ± 7.87 6.42, 23.2	6.65 ± 4.48 1.77, 15.3
Lev/OC $\times 10^{-2}$	0.73 ± 0.66 0.08, 2.29	0.14 ± 0.10 0.08, 0.31	0.84 ± 0.61 0.12, 1.56	1.60 ± 0.67 0.99, 2.29	0.56 ± 0.40 0.11, 1.05
Lev/WSOC $\times 10^{-2}$	1.09 ± 0.97 0.10, 3.46	0.20 ± 0.13 0.10, 0.42	1.25 ± 0.94 0.23, 2.21	2.33 ± 0.90 1.48, 3.46	0.92 ± 0.65 0.13, 1.69
MGA/MLTs	2.18 ± 1.59 0.33, 5.40	0.67 ± 0.43 0.33, 1.33	1.04 ± 0.49 0.41, 1.55	3.60 ± 1.43 1.90, 5.40	3.27 ± 1.17 1.60, 4.75
[e]P/MBTCA	0.62 ± 0.61 0.17, 5.90	3.22 ± 0.62 2.47, 3.89	3.62 ± 1.67 1.52, 5.90	1.68 ± 0.64 0.83, 2.38	1.73 ± 1.07 0.34, 3.32
Carbonaceous components					
Isoprene derived SOC ($\mu gC\ m^{-3}$)	23.7 ± 23.9 2.26, 97.4	51.0 ± 32.4 8.08, 97.4	25.9 ± 17.9 8.54, 45.7	8.52 ± 1.07 7.46, 9.87	11.3 ± 6.80 2.26, 24.9
Isoprene SOC to OC (%)	1.45 ± 1.74 0.21, 6.40	3.56 ± 2.18 1.03, 6.40	1.46 ± 1.38 0.35, 3.48	0.35 ± 0.17 0.21, 0.57	0.57 ± 0.38 0.24, 1.35
Isoprene SOC to total SOC (%)	35.5 ± 15.5 13.5, 71.1	46.6 ± 20.3 26.0, 71.1	38.1 ± 10.4 21.1, 47.3	31.6 ± 7.05 24.0, 39.7	27.9 ± 15.5 13.5, 54.0
Monoterpene SOC ($\mu gC\ m^{-3}$)	40.1 ± 33.3 7.18, 154	62.7 ± 56.5 19.2, 154	40.7 ± 20.0 11.8, 57.7	19.3 ± 5.61 14.0, 25.2	35.5 ± 23.5 7.18, 62.7
Monoterpene SOC to OC (%)	2.0 ± 1.47 0.37, 5.74	3.65 ± 1.58 2.44, 5.74	2.15 ± 1.45 0.48, 3.88	0.87 ± 0.58 0.37, 1.48	1.58 ± 0.84 0.54, 3.13
Monoterpene SOC to total SOC (%)	64.5 ± 15.5 28.9, 86.5	53.4 ± 20.3 28.9, 74.0	61.9 ± 10.4 52.7, 78.9	68.4 ± 7.05 60.3, 76.1	72.1 ± 15.5 46.0, 86.5

[e]P: *cis*-pinonic acid + pinic acid

Table 3. Comparisons of the mean concentration (ng m^{-3}) of anhydrosugars, sugar, and sugar alcohols in Gosan aerosols with those from different sites around the world.

Sampling sites	Sampling type	Sampling time	Anhydro-sugars	Primary sugars	Sugar alcohols	References
Gosan, South Korea	**TSP**	Summer Fall Winter Spring	**3.74** **25.9** **48.0** **15.7**	**22.8** **38.3** **20.2** **90.0**	**14.3** **13.4** **2.60** **7.36**	**This study**
Chennai, India	PM10	Summer Winter	127 134	15.5 11.4	7.44 4.81	Fu et al., 2010b
Mt. Tai, China	TSP	Summer (June)	224	61.1	125	Fu et al., 2012b
Alert, Canada	TSP	Winter Spring	0.32 0.02	1.14 0.18	0.25 0.36	Fu et al., 2009a
Okinawa, western North Pacific	TSP	Summer Autumn Winter Spring	0.93 2.58 6.04 3.44	73.5 56.0 34.4 101	62.9 30.7 6.03 31.2	Zhu et al., 2015a, b
Chichijima, western North Pacific	TSP	Summer Autumn Winter Spring	0.32 0.85 2.40 0.94	32.8 22.0 14.2 24.2	38.6 35.1 3.93 15.5	Verma et al., 2015, 2018
Mt. Hua, China (Non-dust storm)	PM10	April	57.8	92.5	22.4	Wang et al., 2012
Mt. Hua, China (Dust storm)	PM10	April	44.5	162	25.7	Wang et al., 2012
Nanjing, China	PM2.5	Summer Winter	151 (Lev) 268 (Lev)	59.3 42.3	11.8 13.4	Wang and Kawamura, 2005
Beijing, China	PM2.5	Summer Autumn Winter Spring	14.5 129 254 81.4	6.63 17.2 41.5 33.9	3.31 13.7 17.8 12.3	Kang et al., 2018a
Belgrade, Serbia	TSP	Autumn	425 (Lev)	116	98.4	Zangrando et al., 2016
Maine, USA	PM1	May-October	13.9	28	8.31	Medeiros et al., 2006
Crete, Greece	PM10	Year-round	14.4	32.3	6.53	Theodosi et al., 2018